Structure of metal catalysts

John H. Sinfelt

Corporate Research Laboratories, Exxon Research and Engineering Co., Linden, New Jersey 07036

Metal catalysts are technologically very important. Moreover, these materials are intriguing systems for scientific investigation. In general, metal catalysts are highly dispersed materials, i.e., materials with very high surface areas. The study of these materials with chemical probes including chemisorption and selected catalytic reactions, in conjunction with physical methods such as electron microscopy, x-ray diffraction, photoelectron spectroscopy, and extended x-ray absorption fine-structure spectroscopy, has contributed much to our knowledge of their structures. Metal catalysts considered in this article include systems consisting essentially of a single metal component (monometallic catalysts) and also bimetallic systems, this latter group including metal alloys as well as highly dispersed bimetallic clusters.

CONTENTS

I. INTRODUCTION

A catalyst is a substance which accelerates a chemical reaction without being consumed itself in the process. The phenomenon of catalysis is a vital factor in biological processes (Bender and Brubacher, 1973) and also provides the basis for numerous large-scale industrial processes for the refining of petroleum and the manufacture of chemicals (Prettre, 1963). It also plays an important role in environmental problems such as the control of pollutants from automobile exhaust gases. In general, the technological applications of catalysis have developed at a very rapid pace during the twentieth century. Early in this century the Haber process for the synthesis of ammonia from elemental nitrogen and hydrogen was developed (Frankenburg, 1955). The reaction is conducted at high pressure (200–1000 atm) and temperature (about 450°C) over solid iron catalysts, and is the backbone of the fertilizer industry. At about the time of World War II, catalytic cracking of petroleum fractions for the production of gasoline and heating oil assumed a major role in the petroleum industry (Murphree *et al.*, 1943). After World War II the development of higher-compression-ratio automobile engines created a need for gasolines of higher antiknock quality, and the catalytic reforming process was developed to fill the need. Catalysts containing precious metals such as platinum are employed in the reforming process (Haensel, 1949a, 1949b; Haensel and Donaldson, 1951). Catalytic cracking and reforming are involved in the processing of millions of barrels of petroleum per day. Catalysts are also used extensively in commercially important processes for the manufacture of polymers and a wide variety of chemicals.

Catalytic processes are commonly divided into two categories, homogeneous and heterogeneous (Sinfelt, 1977b). The former refer to processes in which the catalyst and reactants are present in a single phase, as in a solution. In heterogeneous catalysis, by contrast, the reactants and catalyst are present in separate phases, a common example comprising reactants in a vapor phase in contact with a solid catalyst (Thomson and Webb, 1968). In general, catalytic processes involve a sequence of steps in which the active catalytic entities participating in the steps are continually being regenerated, so that the catalyst is used over and over in the formation of product molecules from reactants. We refer to such a sequence of steps as a closed sequence (Boudart, 1968). In the case of heterogeneous catalysis at the surface of a solid, the active catalyst entity is a site on the surface or a complex of the site with a reactant molecule. For the purpose of illustration we might visualize a chemical reaction $A+B \rightarrow C$ to proceed by a sequence of steps of the following type:

$$A+S \rightarrow A\text{—}S\,,$$

$$A\text{—}S+B \rightarrow C+S\,.$$

The molecule A is adsorbed on a site S to form a surface complex A—S, which then reacts with a molecule of reactant B to form the product molecule C and regenerate the site S. This simple sequence illustrates features common to all catalytic processes, namely, the generation of a reactive intermediate from the reactant, the transformation of the intermediate to a product, and the regeneration of the active catalyst site (Rideal, 1968).

An intriguing aspect of catalysis is the specificity observed. In heterogeneous catalysis at a solid surface, it has long been known that the chemical constitution of

*This article is based on an invited paper presented at the March 1978 meeting of the American Physical Society on the occasion of the author's receipt of the APS International Prize for New Materials. The author was cited for his outstanding contributions to the field of heterogeneous catalysis leading to the synthesis and characterization of a new class of catalytic materials based on the concept of bimetallic clusters.

the surface determines its catalytic properties. If the role of the surface were limited to its ability to concentrate reactants in an adsorbed layer, one would expect any high-surface-area solid to serve as a catalyst for a given reaction. Consideration of a couple of examples shows clearly that this simple view does not suffice. Thus silver catalysts are unique in their ability to catalyze the partial oxidation of ethylene to ethylene oxide, $2C_2H_4 + O_2 \rightarrow 2C_2H_4O$ (Voge and Adams, 1967). On other solid catalysts, the ethylene undergoes predominantly complete oxidation to carbon dioxide and water. In this example a change in the catalyst actually leads to a marked change in the distribution of reaction products, as a result of the different catalysts having markedly different effects on alternative reaction paths. In some cases the observed reaction product is the same on a number of catalysts, but the specific activity (reaction rate per unit surface area or per surface site) varies markedly. A good example is the catalytic hydrogenolysis of ethane to methane $C_2H_6 + H_2 \rightarrow 2CH_4$ on metals, where the specific activity of osmium is almost eight orders of magnitude higher than that of platinum (Sinfelt, 1973a, 1974a). These examples demonstrate very clearly that the chemical nature of the surface is highly important in heterogeneous catalysis.

For catalysis to occur at a surface, chemisorption of at least one reactant is generally required. The reactant molecule is activated in the chemisorption step, which is sensitive to the chemical nature of the surface. In general, catalytic activity is related to the strength of adsorption of a reactant on the surface. Maximum catalytic activity results when chemisorption of the reactant is fast but not too strong. If the adsorption bond is too strong, the catalyst will tend to be highly covered by reactant species which are not readily transformed or by product species which do not desorb readily from the surface. At the other extreme, if the adsorption bond is very weak, the catalytic activity may be severely limited by a low rate of chemisorption, since the activation energy for chemisorption commonly increases as the heat of adsorption decreases. Optimum catalytic activity corresponds in general to some intermediate strength of adsorption between these extremes. In the case of metal catalysts, this optimum condition is frequently found among the metals of Group VIII of the Periodic Table, and consequently these metals are particularly important in catalysis (Sinfelt, 1975).

In heterogeneous catalytic processes involving solid catalysts the reaction is commonly conducted in a flow system in which the reactant stream is passed through a vessel containing a bed of catalyst granules or pellets. Transport of reactant molecules from the bulk fluid phase to the active surface of the catalyst, and of product molecules away from the surface into the fluid stream, are important steps in the overall catalytic process, and can sometimes be the rate-limiting steps (Weisz and Prater, 1954; Wheeler, 1955). In studies with the goal of obtaining information on the true kinetics of the chemical transformation at the surface, care must be taken in the design of the experiments to minimize transport limitations. This problem is commonly handled by a consideration of such factors as the size and porosity of the catalyst granules or pellets and the fluid velocity in the reactor. Because of the heat of reaction generally associated with chemical change, it is also necessary to consider problems involving the transport of heat and the possibility of nonisothermal conditions in a reactor.

The introduction here has been intended to give only a very general outline of some of the main features of catalytic phenomena. In the present article our attention is confined to the area of heterogeneous catalysis by metals. In particular, we will be concerned primarily with the metal catalysts themselves and only in a secondary manner with the reactions which occur on such catalysts. We begin with a general discussion of the nature of metal catalysts, which includes material on preparative methods. We then consider the structures of monometallic and bimetallic catalyst systems, the latter including metal alloys and supported bimetallic clusters.

II. NATURE OF METAL CATALYSTS

Catalysts of practical interest are characterized by a high specific surface area (i.e., a high surface area per unit mass of material). The catalyst mass may consist exclusively of a finely divided metal, or the metal may be dispersed on the surface of a suitable carrier material. In the latter case the carrier is commonly a high-surface-area form of a refractory oxide such as alumina or silica. When a carrier is employed, we refer to the metal as a supported metal.

A. Nonsupported metals

Nonsupported metal catalysts may be prepared by a variety of methods (Sinfelt, 1972a). One method involves the direct reduction of a suitable compound of the metallic element in a stream of hydrogen. The type of compound employed as a starting material depends on the particular metal involved. In the case of the Group VIII metal rhodium, for example, metal granules can be prepared using rhodium trichloride (Yates and Sinfelt, 1967). For nickel and copper the starting materials are frequently hydroxides, carbonates, or basic carbonates. These materials are often prepared as finely divided precipitates from solutions of the metal nitrates, with the use of a precipitating agent such as sodium hydroxide or ammonium bicarbonate. The precipitate is then commonly heated in air at a temperature of 250°–350°C to form a metal oxide, which is then reduced to the metal in flowing hydrogen. Heating mixtures of hydroxides (Emmett and Skau, 1943) or basic carbonates (Best and Russell, 1954), formed by coprecipitation from solution, gives mixed oxides which on reduction yield metal alloys. Nickel–copper alloys for catalytic studies have frequently been prepared in this manner (Hall and Emmett, 1958, 1959; Sinfelt *et al.*, 1972). Depending on the conditions used, nonsupported metal catalysts prepared by the procedures outlined in this paragraph may have surface areas of the order of 1–10 m^2/g.

Another method of preparation of nonsupported metal catalysts is exemplified by the reduction of Group VIII metal salts with sodium borohydride to yield finely

divided black precipitates (Brown and Brown, 1962). This method, with extensive washing of the precipitates to ensure thorough removal of sodium and boron impurities and subsequent hydrogen treatment of the precipitates at 300°C to assure complete reduction, has been employed in the preparation of platinum, palladium, rhodium, and ruthenium catalysts (Carter *et al.*, 1971). The surface areas of the metals ranged from 3.7 to 30.5 m^2/g. The method has also been employed in the preparation of metal alloy catalysts by reduction of solutions of mixed halides of the metals (McKee, 1965, 1967).

An interesting type of nonsupported metal catalyst may be prepared from binary alloys of a catalytically active metal and a second metal by leaching the latter from the alloy with suitable reagents. The resulting material is commonly called a skeletal metal because of the very open, skeletonlike structure. The classic example of this type of catalyst is Raney nickel, which is prepared by leaching away the aluminum in a nickel-aluminum alloy with a concentrated solution of sodium hydroxide (Raney, 1940). The resulting material is washed thoroughly and then dried. The drying step is commonly conducted *in vacuo* or in an inert atmosphere, since the metal is highly pyrophoric. Raney nickel catalysts with surface areas as high as 76 to 87 m^2/g have been reported (Watt *et al.*, 1951; Kokes and Emmett, 1959). Such catalysts are commonly used for hydrogenation reactions in the liquid phase.

B. Supported metals

Supported metal catalysts are widely used in industrial processes. The carrier on which the metal is supported may be visualized as a porous material with a huge amount of surface contained in pores with diameters in the range of 20 to 400 Å. The metal then exists as extremely small aggregates, with sizes commonly in the range of 10–100 Å, residing on the walls of the pores. These highly dispersed metal entities have often been regarded as very small crystallites of approximately spherical shape, but there is evidence that they may also exist in the form of thin raftlike structures (Prestridge *et al.*, 1977). In general, we shall refer to these highly dispersed entities as metal clusters. A supported metal catalyst will in general have a distribution of cluster sizes and possibly exhibit metal clusters with different shapes. The specific surface areas of supported metals are generally much higher than those of nonsupported metals, and they are more resistant to decline resulting from agglomeration (sintering) of the metal. The stability is extremely important in high-temperature industrial applications, since it is vital for the maintenance of catalytic activity and can be the critical factor in limiting the useful life of the catalyst.

A number of methods can be employed in the preparation of supported metal catalysts (Sinfelt, 1972a). Impregnation and precipitation methods are the most common. In the former, a solution in which the solute is a salt or other compound of the metal is contacted with the carrier. Frequently, the amount of solution employed is just enough to wet the carrier. The solvent, generally water, is removed by drying, and the resulting material consists of the carrier with solute deposited on it. The drying step is sometimes followed by a higher-temperature heat treatment called calcination. Reduction of the material deposited on the carrier to the metallic form, usually with a stream of hydrogen at elevated temperature (300°–550°C), is the final step in the preparation. The material then consists of an assembly of small metal clusters dispersed over the carrier surface. A typical example is the preparation of nickel on silica, in which an aqueous solution of nickel nitrate is employed as the impregnating solution (Yates *et al.*, 1964). The final reduction step is conducted in hydrogen at about 400°C. In the preparation of supported platinum catalysts, a solution of chloroplatinic acid is commonly used for the impregnation, and the final reduction temperature is usually about 500°C. An impregnating solution containing both chloroplatinic and chloroiridic acids is used for the preparation of platinum–iridium bimetallic clusters (Sinfelt, 1976b). Similarly, an aqueous solution of ruthenium trichloride and copper nitrate is used in the preparation of bimetallic clusters of ruthenium and copper (Sinfelt, 1973b).

In precipitation methods for preparing supported metal catalysts, a hydroxide or carbonate of a metal may be precipitated from a solution of a metal salt onto a carrier material suspended in the solution. For example, in the preparation of a nickel on silica catalyst, nickel hydroxide may be precipitated onto silica by addition of alkali to a solution of nickel nitrate in which silica is slurried. The preparation is completed by reduction of the dried, calcined material in hydrogen at 400°–450°C. A procedure termed coprecipitation, in which the carrier is precipitated simultaneously with a compound of the metal, is sometimes used in preparing supported metal catalysts. Thus a nickel on alumina catalyst may be prepared by addition of ammonium bicarbonate to an aqueous solution of nickel and aluminum nitrates (Taylor and Sinfelt, 1967). The resulting precipitate is separated from solution by filtering, after which it is dried, calcined, and finally reduced in hydrogen at about 350°–500°C. The choice of a method of preparation depends on the particular catalyst and application, and in general involves considerations of detail beyond the scope of this article.

III. MONOMETALLIC CATALYSTS

The previous section of this article was concerned with a general description of metal catalysts, including methods of preparation. In this section we give a more detailed discussion of the dispersion and structure of metal catalysts based on investigations of gas adsorption and on studies employing a variety of physical methods. The discussion in this section is limited to catalysts in which the metal component consists of a single metallic element. We use the term "monometallic catalysts" in classifying them.

A. Gas adsorption measurements of metal dispersion

The surface areas of metal catalysts are most commonly determined by gas adsorption measurements. In cases where the active metal component constitutes the

entire catalyst mass, so that the total surface area and the metal surface area are identical, the classical low-temperature physical (multilayer) adsorption method of Brunauer, Emmett, and Teller (1938), known as the BET method, may be employed. The method involves the measurement of an adsorption isotherm for nitrogen or one of the rare gases on the catalyst, often at the boiling point of nitrogen (77°K). From the isotherm one can determine, with the aid of the BET theory, the number of molecules required to give a monolayer. Multiplication of this quantity by the cross-sectional area of the adsorbed molecule (16.2 $Å^2$ in the case of nitrogen) yields the surface area of the catalyst.

Since physical adsorption is nonspecific with respect to the nature of the surface, and hence yields information on total surface area, it cannot be used to determine the surface area of the metal in a supported metal catalyst. In such catalysts the measured surface area would include the uncovered area of the carrier as well as that of the metal. Frequently the metal surface area is only a small fraction of the total. To determine the surface area of the metal component, one needs a selective method in which gas is adsorbed on the metal but not on the carrier. One must therefore use chemisorption rather than physical adsorption and adopt a gas and conditions such that the chemisorption is restricted to the metal component (Emmett and Brunauer, 1937; Spenadel and Boudart, 1960; Adler and Keavney, 1960; Gruber, 1962). This means employing temperatures too high for physical adsorption to occur. For a number of Group VIII metals dispersed on silica or alumina, the use of hydrogen or carbon monoxide at room temperature is generally satisfactory in meeting these requirements (Sinfelt, 1969, 1972a; Sinfelt and Yates, 1967, 1968). Saturation coverage of the metal is attained at very low equilibrium pressures, so that the isotherms are very flat over the range of pressures of the isotherms, commonly 10–200 Torr. This is clearly desirable, since one can then readily determine a saturation (monolayer) value for the amount of adsorbed gas. In the chemisorption of hydrogen on the Group VIII metals, it is a generally accepted view that the hydrogen molecule dissociates into atoms on chemisorption. Results of hydrogen chemisorption studies on a series of rhodium catalysts of varying rhodium concentration are summarized in Fig. 1 (Sinfelt, 1972a) which is based on data of Yates and Sinfelt (1967). The quantity H/M, representing the number of hydrogen atoms chemisorbed per atom of rhodium metal in the catalyst, increases with decreasing rhodium concentration, approaching a limiting value of unity for rhodium concentrations of 1 wt. % and lower. The dispersion, defined as the ratio of surface metal atoms to total metal atoms in the catalyst, thus increases with decreasing rhodium concentration, as would be expected for a series of catalysts prepared in the same manner. If the stoichiometry of the hydrogen chemisorption corresponds to one hydrogen atom per surface rhodium atom, the dispersion approaches unity at the lowest rhodium concentrations. This stoichiometry was verified for the 100% rhodium catalyst by determining the number of surface rhodium atoms from a measurement of surface area by low-temperature physical adsorption.

B. Electron microscopy studies

Electron microscopy studies give direct information on the size and shape of particles. High-resolution transmission electron microscopes can be operated with resolutions close to the dimensions of individual atoms. Studies on supported metal catalysts have been successful in demonstrating the presence of metal clusters with diameters of the order of 10 Å. An electron micrograph of a highly dispersed osmium catalyst is shown in Fig. 2. Data on the distribution of the os-

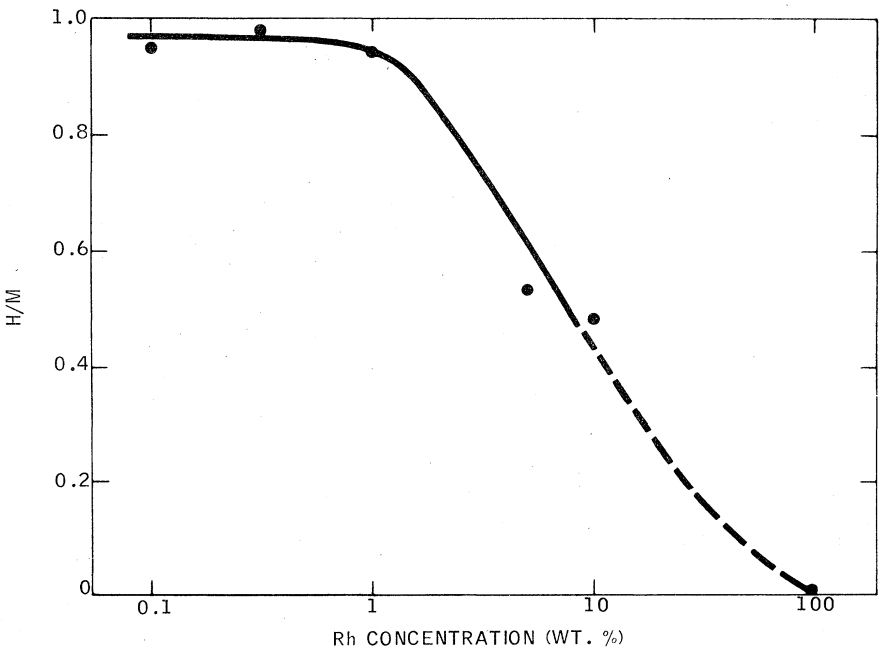

FIG. 1. Hydrogen chemisorption on a series of rhodium catalysts of varying rhodium concentration. The catalysts containing 0.1% to 10% rhodium are silica-supported catalysts. The quantity H/M refers to the number of hydrogen atoms adsorbed per atom of rhodium metal in the catalyst. All of the catalysts were reduced in hydrogen at 450°C in their preparation. The chemisorption data were obtained at room temperature (Sinfelt, 1972a; Yates and Sinfelt, 1967).

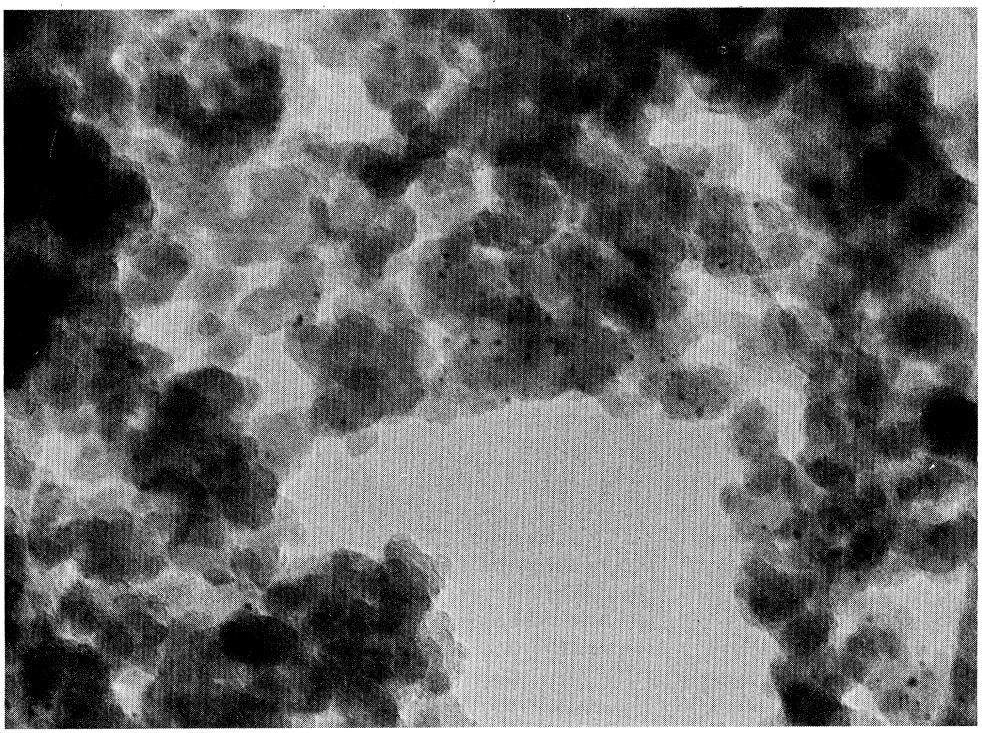

FIG. 2. Electron micrograph of silica-supported osmium catalyst containing 1 wt.% osmium. The osmium clusters (the black dots in the micrograph) are very highly dispersed, with diameters ranging from 5 to 25 Å. The average diameter is 12 Å (Prestridge, Via, and Sinfelt, 1977).

mium cluster sizes in this catalyst and corresponding data on the ruthenium clusters in a silica-supported ruthenium catalyst (Prestridge, Via, and Sinfelt, 1977) are shown in Figs. 3 and 4. Hydrogen and carbon monoxide chemisorption measurements on the catalysts indicated that the dispersion of the osmium was close to unity, while that of the ruthenium was about 0.4–0.5 (Sinfelt, 1973b). The data on the osmium catalyst in Fig. 3 indicate osmium cluster diameters in the range of 5–25 Å, with an average diameter of 12 Å. The electron microscopy data provide excellent confirmation of the extremely high dispersion of the osmium indicated by gas chemisorption measurements. Similar agreement between electron microscopy and gas chemisorption data on highly dispersed metals has been noted for platinum (Wilson and Hall, 1970) and rhodium (Prestridge and Yates, 1971).

The data on the distribution of sizes of the ruthenium clusters in Fig. 4 show a broader distribution than was observed for the osmium catalyst. The diameters of the ruthenium clusters range from 10 to 100 Å, and the average diameter is 36 Å. If the ruthenium clusters were spheres (or cubes), the ruthenium dispersion corresponding to the average cluster diameter of 36 Å would be about 0.3 instead of the value of 0.4–0.5 obtained by chemisorption. The higher value of dispersion indicated by the chemisorption data suggests the possibility that some of the ruthenium clusters are present in the form of very thin raftlike structures. The fraction of the atoms present as surface atoms

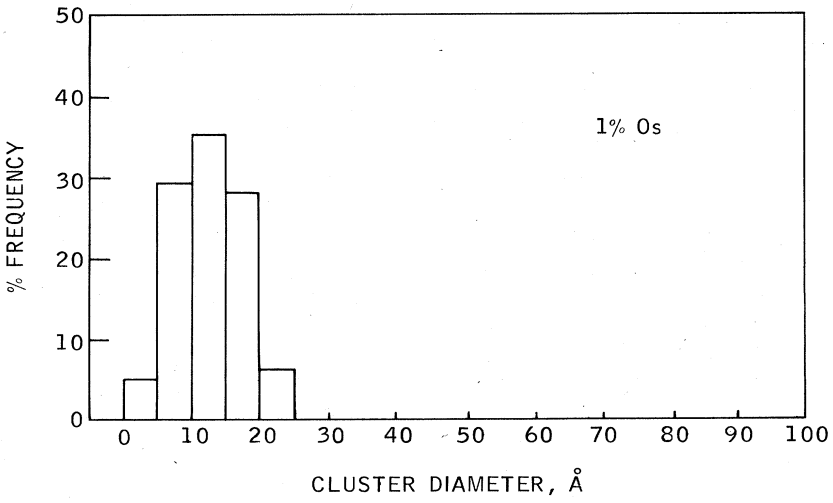

FIG. 3. Distribution of sizes of the osmium clusters in the catalyst of Fig. 2 (Prestridge, Via, and Sinfelt, 1977).

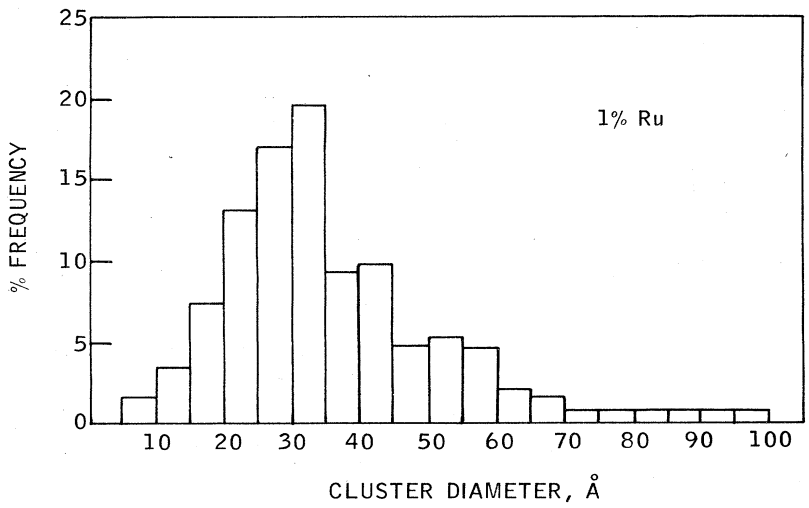

FIG. 4. Distribution of sizes of the ruthenium clusters in a silica-supported ruthenium catalyst containing 1 wt. % ruthenium. The average diameter of the clusters is 36 Å (Prestridge, Via, and Sinfelt, 1977).

would be higher for a thin raftlike cluster than for a spherically symmetrical cluster. A study of the original electron micrographs of the ruthenium catalyst provides support for the suggestion that some of the ruthenium is present in the form of thin raftlike clusters. The inference about the shape of the ruthenium clusters is drawn from an examination of the contrast of a metal cluster with its immediate surroundings in the micrograph, i.e., with the silica carrier. This contrast arises from differences in scattering of electrons by the cluster and its surroundings. The original electron micrographs of the ruthenium catalyst showed two different types of clusters with regard to the extent of contrast observed. Many exhibited low contrast with their surroundings, while some exhibited very high contrast (i.e., they were much darker than the former). Low contrast was observed for all of the clusters with diameters smaller than 40 Å, while high contrast was observed for clusters with diameters larger than 60 Å. Both low- and high-contrast clusters were observed in the diameter range of 40–60 Å. We have concluded that the clusters exhibiting low contrast are extremely thin, and we identify them with the raftlike clusters already mentioned. We have found regions of the micrographs in which the boundary of one cluster located partially under a second cluster can be seen through the latter. In some regions features of the underlying carrier material, such as ridges and boundaries, are clearly visible through such clusters. These observations serve as qualitative indications of the very thin nature of the clusters exhibiting low contrast. It is instructive to look for clusters at the outer boundaries of the carrier material in the micrographs, since one might well expect to obtain a side view of a cluster at such a boundary, and hence arrive at a measure of its thickness. When this was done, we were unable to observe ruthenium clusters at the outer boundaries of the carrier material. Possibly the clusters are too thin to obtain side views in this manner. One would expect a thickness of two atomic layers (about 5 Å) to be detected, especially since clusters of ruthenium or osmium with lateral dimensions of this magnitude are indeed observed on regions of the carrier away from the outer boundaries of the sample. Thus we suggest that the raftlike clusters may consist of single layers of atoms.

The conclusion from the electron microscopy studies that thin raftlike clusters of ruthenium with diameters as large as 40–60 Å exist on a silica carrier implies a significant interaction between the clusters and the silica. The fact that metal dispersions approaching unity have been observed for a number of Group VIII metals dispersed on silica or alumina, and that the dispersions are maintained on exposure to temperatures as high as 500°C in hydrogen or inert gases (especially when the clusters are dispersed on alumina), attests to the existence of such an interaction. The nature of the interaction is a question of considerable interest in our understanding of supported metal catalysts. In the case of silica-supported ruthenium there may be an interaction between ruthenium atoms of the cluster and the oxygen of the silica.

C. Extended x-ray absorption fine-structure studies

In the absorption of x-rays by matter other than monatomic gases, a plot of absorption coefficient vs x-ray energy exhibits an extended fine structure on the high-energy side of an absorption edge. The fine structure, consisting of fluctuations in the absorption coefficient which extend to energies about 1 KeV beyond the edge, was first considered theoretically many years ago by Kronig (1931, 1932a, 1932b). However, the possibilities of extended x-ray absorption fine structure (EXAFS) as a tool for investigating the structures of noncrystalline materials were not realized for a long time afterwards. The realization began with the work of Lytle (1965, 1966) in the 1960s and has been aided greatly in recent years by advances in methods of data analysis (Sayers *et al.*, 1971; Lytle *et al.*, 1975) and experimental techniques, the latter having been associated primarily with the application of high-intensity synchrotron radiation as an x-ray source (Kincaid, 1975, 1977; Kincaid and Eisenberger, 1975; Eisenberger *et al.*, 1974). The application of EXAFS in catalyst studies is of particular interest (Lytle *et al.*, 1977; Sinfelt *et al.*, 1978), since for a number of very highly dispersed catalysts of technological importance it appears to be the only

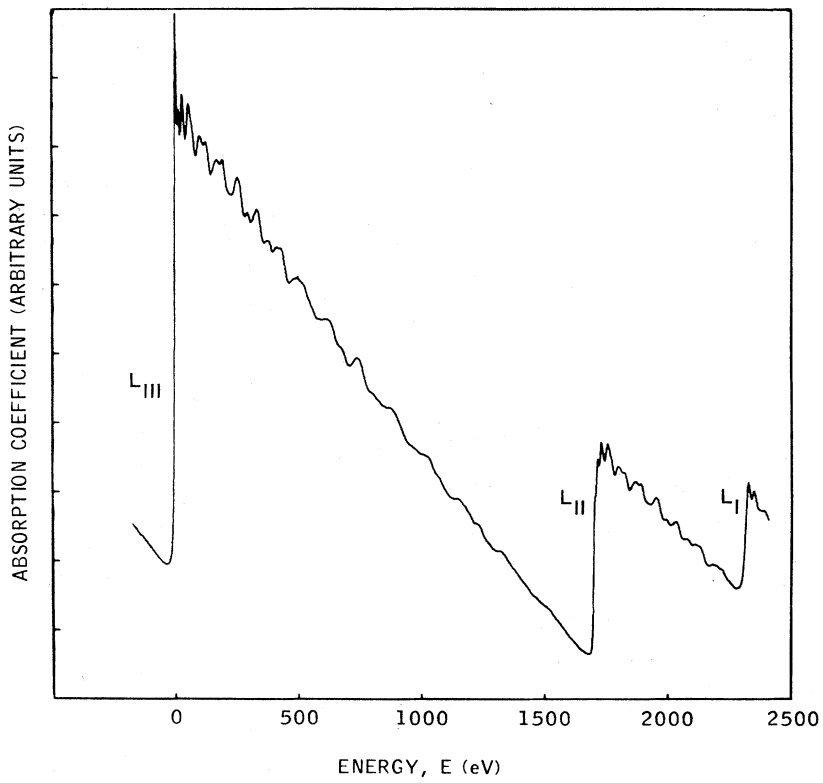

FIG. 5. Typical x-ray absorption spectrum at 100 °K of a 2.5 μ platinum foil in the energy region of the L edges. The energy shown is the energy relative to the L_{III} edge (Sinfelt, Via, and Lytle, 1978).

method capable of yielding detailed structural information. In the case of supported metal catalysts with metal concentrations which are frequently lower than 1 wt.%, the average size of the metal clusters in the catalyst may be of the order of 10 Å. In this situation a classical method such as x-ray diffraction is of little use.

In EXAFS we are concerned with the ejection of an inner core electron from an atom as a result of x-ray absorption. The ejected electron (photoelectron) is characterized by a wave vector K, which is given by the equation

$$K = (2mE)^{1/2}/\hbar , \tag{1}$$

where m is the mass of the electron, $\hbar$ is Planck's constant/2π, and E is the kinetic energy of the photoelectron. The energy E is the difference between the x-ray energy and a threshold energy associated with the ejection of the electron. At the threshold energy, an x-ray absorption spectrum exhibits an abrupt discontinuity known as an absorption edge. A typical spectrum of platinum metal at 100°K is shown in Fig. 5 (Sinfelt *et al.*, 1978). The absorption coefficient is shown as a function of the energy E relative to the L_{III} edge. The data cover a wide enough range of energy to include all three of the characteristic L absorption edges, L_{III}, L_{II}, and L_I, corresponding, respectively, to ejection of photoelectrons from $2p_{3/2}$, $2p_{1/2}$, and $2s$ states. At energies higher than the threshold value corresponding to a particular absorption edge, we note the fluctuations in absorption coefficient which constitute the extended fine structure.

In the analysis of EXAFS data, it is useful to consider a function $\chi(K)$ defined by the equation

$$\chi(K) = (\mu - \mu_0)/\mu_0 , \tag{2}$$

where μ and μ_0 are atomic absorption coefficients characteristic of the absorption associated with the ejection of an inner core electron from an atom. The coefficient μ refers to absorption by an atom in the material of interest while μ_0 refers to absorption by an atom in the free state, both of which are functions of K. The difference between the experimental absorption coefficient at a given energy and a value at the same energy determined by an average background line through the data, i.e., the fluctuation, is proportional to the numerator of Eq. 2. The increase in absorption coefficient at the edge (i.e., the difference between the minimum value at the energy corresponding to the onset of the edge and a value at the same energy obtained by a slight extrapolation of the average background line from the high-energy side of the edge), which we call the step height, is proportional to the denominator μ_0 of Eq. 2. To account for the dependence of μ_0 on K, we determine a hypothetical step height for energies beyond the edge by employing empirical corrections based on the known energy dependence of the absorption coefficient of the element on either side of the edge. A value of $\chi(K)$ at a particular value of K is then determined by dividing the fluctuation by the step height.

Theories of EXAFS (Sayers *et al.*, 1970; Stern, 1974; Ashley and Doniach, 1975; Lee and Pendry, 1975; Lee and Beni, 1977) based on the scattering of an ejected photoelectron by atoms in the coordination shells surrounding the central absorbing atom give an expression

for $\chi(K)$ of the following form

$$\chi(K) = \sum_j A_j(K) \sin[2KR_j + 2\delta_j(K)], \quad (3)$$

where the summation extends over j coordination shells. In this expression, R_j is the distance from the central absorbing atom to atoms in the jth coordination shell and $\delta_j(K)$ is the phase shift. The factor $A_j(K)$ is an amplitude function for the jth shell, and is defined by the expression

$$A_j(K) = (N_j/KR_j^2)F_j(K) \exp(-2K^2\sigma_j^2), \quad (4)$$

where N_j is the number of atoms in the jth shell, σ_j is the root-mean-square deviation of the interatomic distance about R_j, and $F_j(K)$ is a factor accounting for electron backscattering and inelastic scattering.

Fourier transformation of EXAFS data yields a radial structure function (Sayers *et al.*, 1970; Sayers, 1971) which exhibits a series of peaks at $R = R_j' = R_j - a_j$, the variable R representing the distance from the absorber atom. The difference a_j from a value of R_j corresponding to a particular coordination shell arises from the phase shift in Eq. 3. The EXAFS function $\chi(K)$ is commonly multiplied by a weighting factor K^n with $n = 1$ or $n = 3$ before the transform is taken (Stern *et al.*, 1975). Data on $K^3\chi(K)$ vs. K at 100 °K for platinum metal and dispersed platinum catalysts, and Fourier transforms of the data, are shown in Fig. 6 (Sinfelt *et al.*, 1978). The EXAFS fluctuations for the dispersed platinum catalysts are substantially smaller than those for platinum metal. Correspondingly, the magnitudes of the peaks in the Fourier transforms are also smaller (note that the scales in the figures are not the same for the dispersed platinum catalysts and platinum metal). These features are a consequence of a lower average coordination number and/or a higher degree of disorder of the platinum atoms in the dispersed catalysts. The degree of disorder is characterized by the parameter σ_j in Eq. 4. We note that the peaks in the Fourier transforms are located at values of R slightly lower than the true interatomic distances of platinum metal (about 0.12–0.15 Å lower), as a consequence of the phase shift.

In the determination of structural parameters from

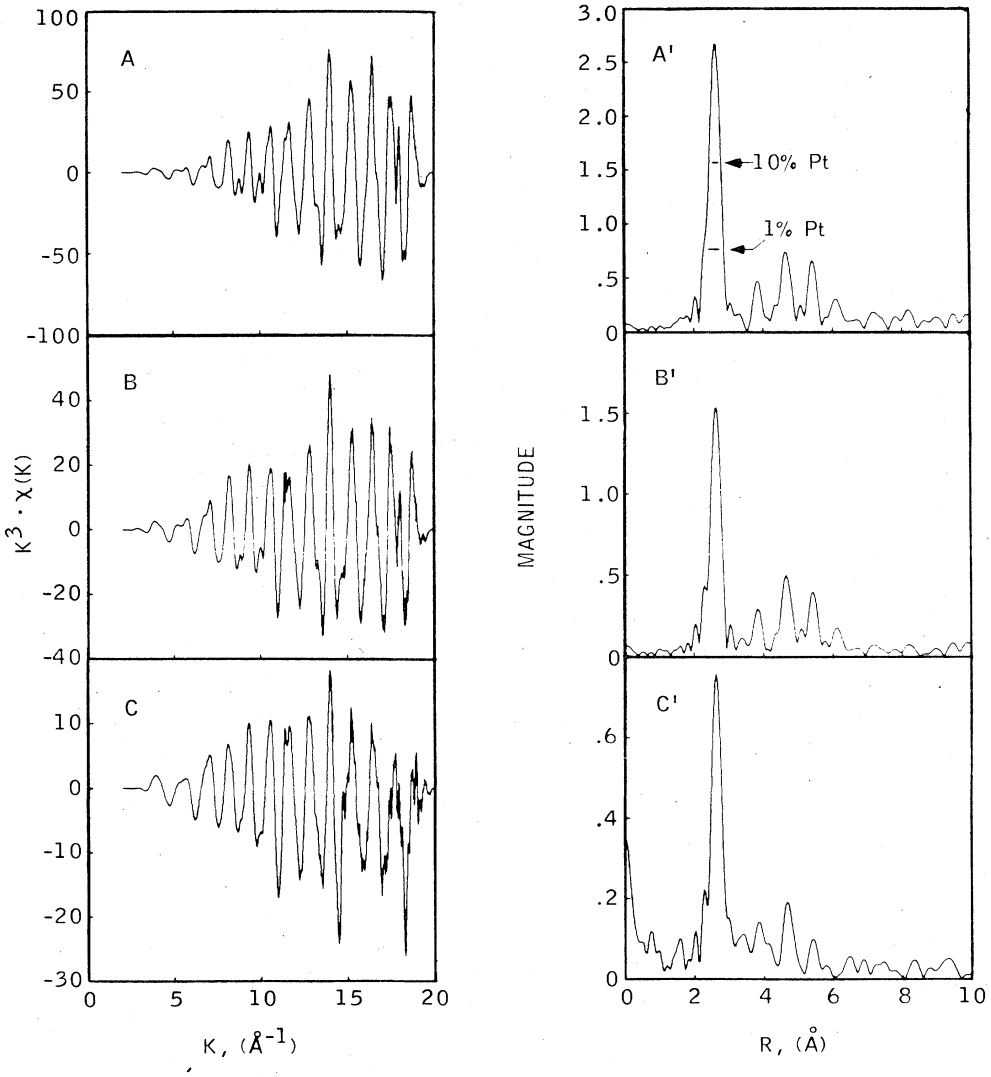

FIG. 6. Normalized L_{III} EXAFS data, $K^3\chi(K)$ vs K at 100 °K, and the corresponding Fourier transforms showing the magnitude of the transform as a function of radial distance R: (A, A') platinum foil; (B, B') 10% platinum catalyst; (C, C') 1% platinum catalyst. Note the different scales on the ordinates in the different parts of the figure. In part A' the arrows indicate the magnitudes of the main peaks for the 10% and 1% platinum catalysts, obtained from parts B' and C' of the figure. The platinum catalysts consist of platinum clusters dispersed on silica (Sinfelt, Via, and Lytle, 1978).

EXAFS data, it is useful to obtain an inverse Fourier transform of the radial structure function over a range of R encompassing a single peak corresponding to a particular coordination shell. This procedure determines the contribution to EXAFS arising from that shell. Thus a Fourier transform over a range of R encompassing only the main peak in the transform (which corresponds to the first coordination shell) yields the function $K^n\chi_1(K)$. If we consider EXAFS due to scattering from atoms in the first coordination shell alone, Eq. 3, after multiplication by the factor K^n, reduces to the simpler expression

$$K^n\chi_1(K) = K^n A_1(K)\sin[2KR_1 + 2\delta_1(K)] , \quad (5)$$

where the subscript 1 refers to the first coordination shell. The amplitude function $A_1(K)$ is given by the equation

$$A_1(K) = (N_1/KR_1^2)F_1(K)\exp(-2K^2\sigma_1^2) . \quad (6)$$

To obtain information on the parameters N_1, R_1, and σ_1 for the highly dispersed platinum clusters in the 1% platinum catalyst of Fig. 6 (platinum dispersion by hydrogen chemisorption estimated to be about 0.9), we begin by analyzing EXAFS data on platinum metal, for which values of N_1 and R_1 are known. The amplitude function $A_1(K)$ in Eqs. 5 and 6 is obtained from the values of the maxima and minima in the function $K^n\chi_1(K)$ derived from the experimental data in the manner just described. For values of K other than those corresponding to maxima and minima, the values of $A_1(K)$ are obtained by interpolation. The function $A_1(K)$ for the catalyst is derived from the EXAFS data in the same way that it was obtained for platinum metal. If the function $F_1(K)$ is the same for platinum metal and the platinum clusters in the catalyst, the logarithm of the ratio of $A_1(K)$ values for the catalyst and platinum metal is a linear function of K^2. From the intercept of a plot of the logarithm of the ratio vs. K^2, we can then determine the ratio of the coordination number N_1 of the platinum atoms in the catalyst to that of the atoms in the bulk metal. When this is done, the value of N_1 for the catalyst is found to be 60% of the value for the bulk metal (Sinfelt *et al.*, 1978). Since $N_1 = 12$ for bulk platinum, we have a value of 7 for the catalyst (with an estimated uncertainty of ±2). From the slope of the plot we obtain a value for $\Delta\sigma_1^2$, which is the difference between σ_1^2 values for the catalyst and platinum metal. In this way we learn that the value of σ_1 is higher for the catalyst than for the bulk metal. The finding that the average coordination number of the platinum atoms in the catalyst is lower than the coordination number for platinum metal is reasonable, since most of the platinum atoms in the catalyst are surface atoms. Such atoms are characterized by lower coordination numbers than are the interior atoms in a crystal, and the difference is even more pronounced for very small clusters where a substantial fraction of the surface atoms may exist at edges and corners.

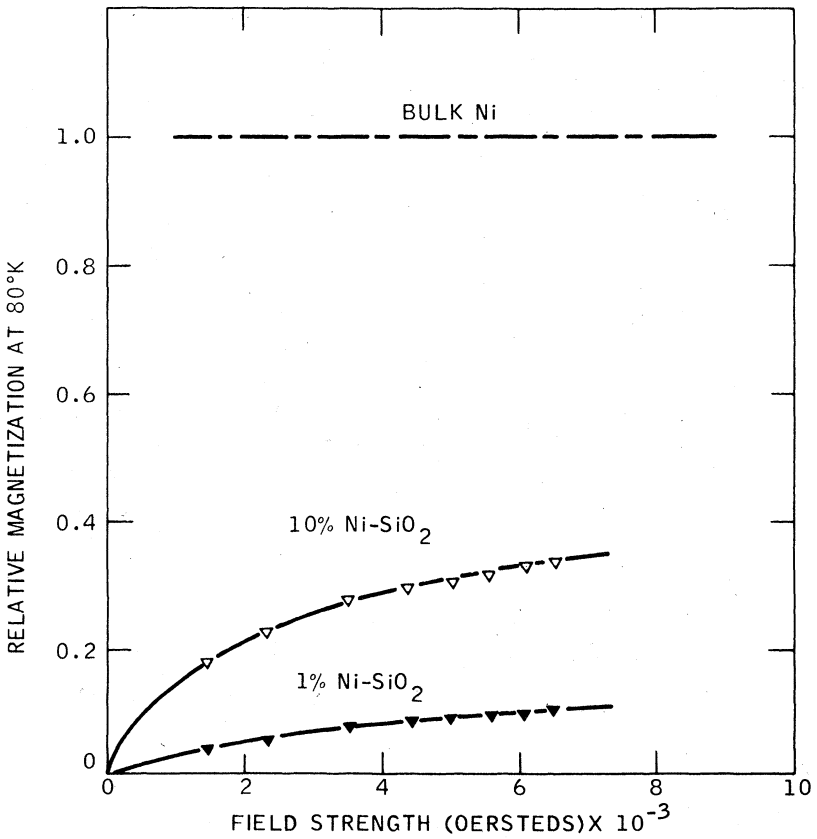

FIG. 7. Comparison of the magnetization of silica-supported nickel catalysts with that of bulk nickel. The catalysts were reduced in hydrogen at 370 °C in their preparation and were subsequently evacuated at 370 °C prior to magnetic measurements (Sinfelt, 1969).

D. Magnetic studies

Magnetic studies provide another approach to the characterization of catalytic materials (Selwood, 1956, 1962). In the case of catalysts containing clusters (crystallites) of a metal which is normally ferromagnetic, the dependence of the magnetic properties on the size of the metal clusters is of particular interest. Figure 7 compares the magnetization of silica-supported nickel clusters in catalysts containing 1% and 10% nickel with the magnetization of bulk nickel (Sinfelt, 1969, 1974b). The relative magnetization, defined as the ratio of the magnetization of the nickel in the material of interest to that of bulk nickel, is shown as a function of field strength at a temperature of 80 °K. The magnetization of the nickel in the nickel–silica catalysts is very much lower than that of bulk nickel and exhibits a dependence on field strength, and also on temperature, which is not typical of a ferromagnetic metal. The magnetic behavior can be described by a theory identical to the classical Langevin treatment of atomic paramagnetism, except that the theory is concerned with the magnetic moments of small ferromagnetic particles (with sizes lower than about 150 Å) rather than with the moments of single atoms. Although the particles are very small, the number of atoms in a particle may be as high as 10^5 and hence the moments are large compared to that of a single atom. The term "superparamagnetism" is thus employed in discussions of the magnetic behavior of such particles (Bean and Livingston, 1959).

A low field approximation of the theory of superparamagnetism leads to the following equation for the particle volume v

$$v = (3kT/I_{sp})(M/I_{sp}H) . \tag{7}$$

In this expression, k is Boltzmann's constant, T is the absolute temperature, I_{sp} is the spontaneous magnetization, and M is the magnetization at field strength H. In the use of Eq. 7 to estimate values of v for the nickel clusters in the catalysts of Fig. 7, we assume as a first approximation that I_{sp} is the same for bulk nickel and the highly dispersed nickel in the catalysts, and we identify the relative magnetization with the quantity M/I_{sp}. Since Eq. 7 is strictly applicable only when the field strength approaches zero, we equate the quantity $M/I_{sp}H$ in the equation with the initial slopes of the curves for the catalysts in Fig. 7. If we take the cube root of v obtained from Eq. 7 as the nickel cluster size, we obtain values of 12 and 24 Å, respectively, for the 1% and 10% nickel catalysts. It should be appreciated that such catalysts will in general have a distribution of cluster sizes and that the use of low field data in Eq. 7 emphasizes the contribution of the larger clusters to the magnetization. The contribution of the smaller clusters becomes more important in determining the approach to magnetic saturation at very high fields. Nevertheless, Eq. 7 is useful for comparing catalysts such as the two nickel catalysts of Fig. 7, and for obtaining information on changes in a catalyst as a result of exposure to conditions (such as high temperatures) which could affect the dispersion of the metal.

IV. BIMETALLIC CATALYSTS

Bimetallic catalysts have played an important role in the field of heterogeneous catalysis. They have long been of interest for fundamental investigations of catalysis by metals, and in recent years have also been demonstrated to be of great importance in technological applications. Systems of interest include metal alloys and bimetallic cluster catalysts. The latter category includes combinations of metals which do not alloy in the normal sense, i.e., combinations which exhibit extremely low miscibility in the bulk.

A. Metal alloy catalysts

Metal alloys first attracted significant attention in catalysis in investigations of the relationship between the catalytic activity of a metal and its electronic structure (Schwab, 1950; Dowden, 1950). The approach was based on the electronic structure of a metal crystal as a whole rather than on the localized structures of individual surface atoms. Thus, for example, the high catalytic activity of nickel relative to copper was related to the incompletely filled d band of the nickel. Nickel and copper are both face-centered cubic metals which can be combined to form alloys (solid solutions). The alloys can be characterized by x-ray diffraction, as illustrated by data in Fig. 8 on lattice constants of nickel-copper alloys (Sinfelt *et al.*, 1972). Figure 8 includes data on a series of nickel-copper catalysts prepared by a method described in a previous section of this article. The surface areas of these catalysts were about 1 m^2/g. Data on a number of metallurgical preparations (Coles, 1956) are also included for comparison. The variation of lattice constant with composition is approximately linear. When copper is alloyed with nickel, the magnetization of the alloy is lower than that of pure nickel, as shown by the data in Fig. 9 (Sinfelt *et al.*, 1972). The points in Fig. 9 are data on the same nickel-copper catalysts used in obtaining the x-ray diffraction data in the previous figure. The solid line in Fig. 9 represents comparison data on metallurgical preparations (Ahern *et al.*, 1958). The ferromagnetism disappears at a composition of approximately 60 at.% copper, which corresponds to a completely filled d band. The early studies on nickel–copper alloy catalysts were thus concerned with relating catalytic activity to alloy composition, as a way of following changes in catalytic activity with progressive filling of the d band of the metal. This approach of emphasizing collective electron properties in metal catalysis has not proved to be fruitful. The accumulation of experimental data on chemisorption and catalysis has made it increasingly clear that localized properties of surface metal atoms are very important (Sinfelt, 1977a). In nickel–copper alloys the atoms retain their inherent chemical differences, although bonding properties of the metal atoms are probably altered to some extent. Current studies of the electronic factor in catalysis by metal alloys are being pursued from this point of view (Sachtler and van der Plank, 1969).

Early studies of the catalytic properties of alloys were concerned with the activity of a catalyst for a particular reaction, which was commonly a simple hydro-

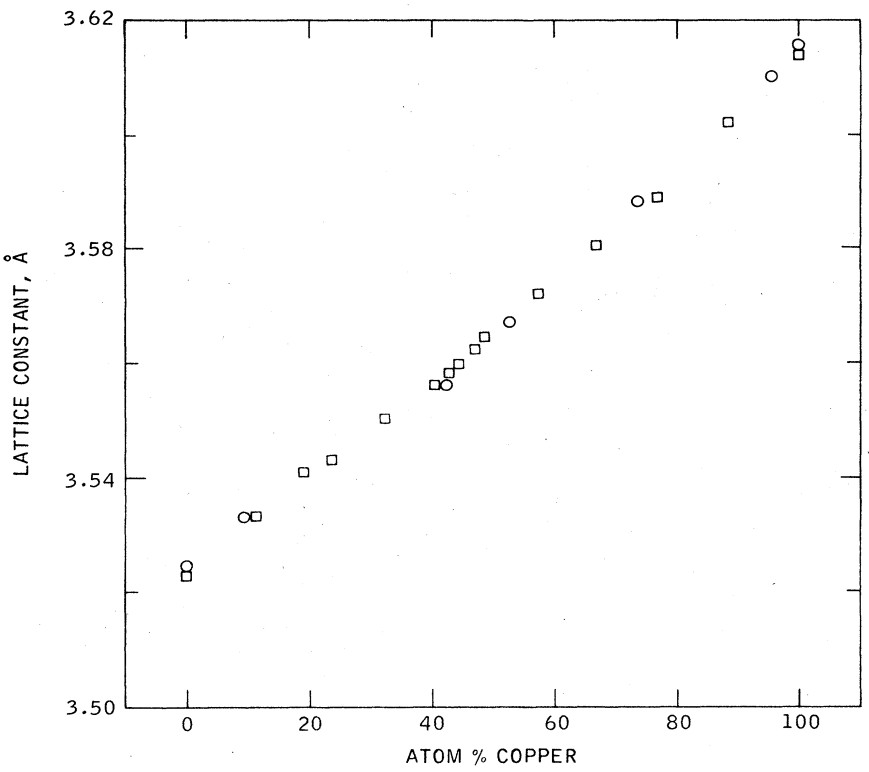

FIG. 8. Lattice constants of nickel–copper alloys as a function of composition (Sinfelt *et al.*, 1972). The circles represent data on low-surface-area (~1 m^2/g) catalysts; the squares are the data of Coles (1956) on metallurgical specimens.

genation reaction of an unsaturated hydrocarbon. The possibility that the effect of alloying depends on the type of reaction has only recently received any attention (Sinfelt *et al.*, 1969, 1971, 1972, 1976; Sinfelt, 1973b; Ponec and Sachtler, 1972; Beelen *et al.*, 1973). The importance of considering the type of reaction is strikingly illustrated by recent work on nickel–copper alloy catalysts in which two different reactions were investigated, the hydrogenolysis of ethane to methane and the dehydrogenation of cyclohexane to benzene.

$$C_2H_6 + H_2 \rightarrow 2CH_4,$$

$$C_6H_{12} \rightarrow C_6H_6 + 3H_2.$$

As shown by the data in Fig. 10, the effect of copper on

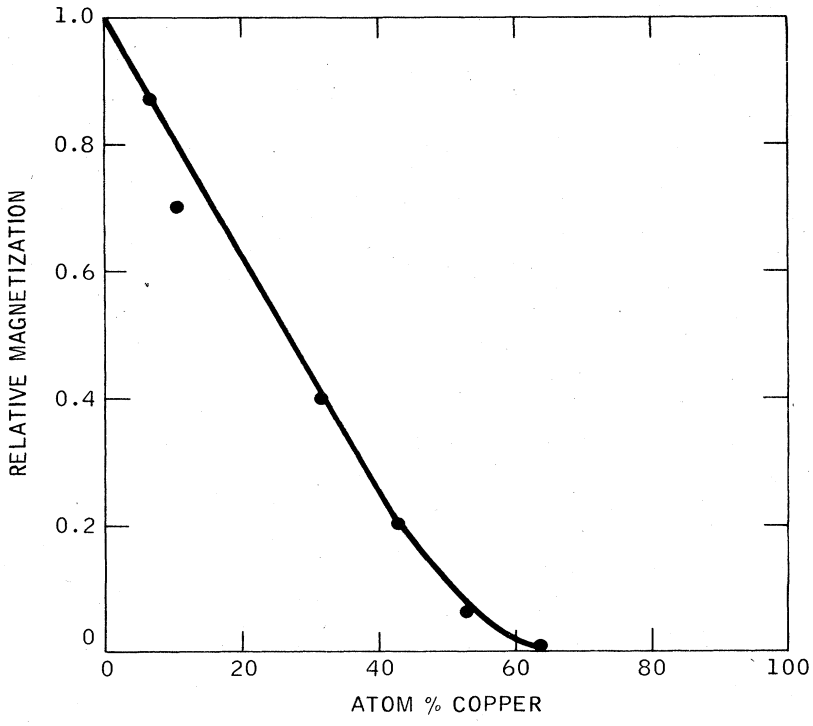

FIG. 9. Magnetization of nickel–copper alloys as a function of composition (Sinfelt *et al.*, 1972). The points represent data on the catalysts of Fig. 8; the curve represents data (Ahern *et al.*, 1958) on metallurgical specimens.

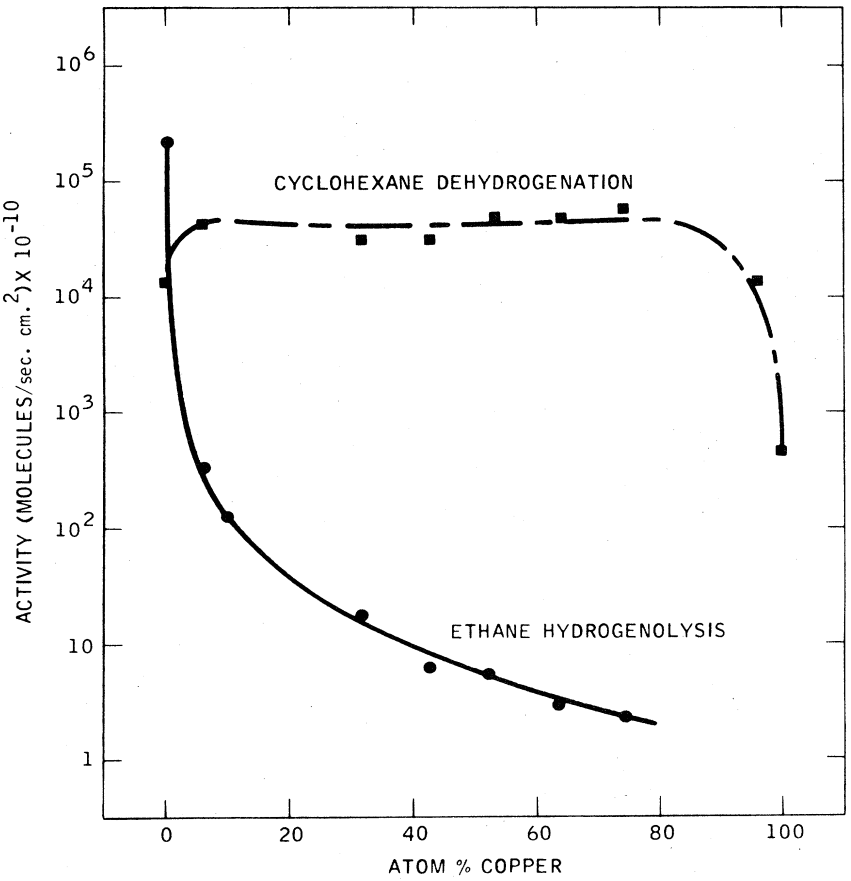

FIG. 10. Activities of Ni–Cu catalysts for the hydrogenolysis of ethane to methane and the dehydrogenation of cyclohexane to benzene. The activities refer to reaction rates at 316 °C. Ethane hydrogenolysis activities were obtained at ethane and hydrogen pressures of 0.030 and 0.20 atm, respectively. Cyclohexane dehydrogenation activities were obtained at cyclohexane and hydrogen pressures of 0.17 and 0.83 atm, respectively (Sinfelt *et al.*, 1972).

the catalytic activity of nickel is very different for these two reactions. In the case of ethane hydrogenolysis, addition of only 5 at.% copper to nickel decreases catalytic activity by three orders of magnitude. Further addition of copper continues to decrease the activity. However, the activity of nickel for dehydrogenation of cyclohexane is affected very little over a wide range of composition, and actually increases on addition of the first increments of copper to nickel. Only as the catalyst composition approaches pure copper is a marked decline in activity observed.

In discussing the results of Fig. 10, we first consider the possibility that the surface composition of the nickel–copper alloy may differ from the bulk composition. Evidence for such a difference in the case of nickel–copper alloys has been obtained from hydrogen chemisorption studies, and is based on the observation that strong chemisorption of hydrogen does not occur on copper. The addition of only a few percent of copper to nickel decreases the amount of strongly chemisorbed hydrogen severalfold, suggesting that the concentration of copper in the surface is much greater than in the bulk (van der Plank and Sachtler, 1967; Cadenhead and Wagner, 1968; Sinfelt *et al.*, 1972). Typical data are shown in Fig. 11 (Sinfelt, 1974a). The findings are consistent with data on surface composition obtained by Auger spectroscopy (Helms, 1975).

In the hydrogenolysis of ethane, kinetic studies of the reaction over the metals of Group VIII have led to the hypothesis of a hydrogen deficient surface intermediate, C_2H_x, being involved in the reaction (Cimino *et al.*, 1954; Sinfelt, 1964, 1972c, 1973a). It is visualized that the intermediate is bonded to more than one surface metal atom, as illustrated for an intermediate of composition C_2H_2 by the following structure

$$\underset{**}{HC}\!-\!\underset{**}{CH}$$

The asterisks represent bonds between the carbon atoms and active metal surface atoms. Such an intermediate would require sites comprising "multiplets" of adjacent active metal atoms. The term multiplet is taken from the work of Balandin (1958). If the active metal atoms are diluted with inactive metal atoms in the surface, the concentration of active multiplets will decline sharply. For the nickel–copper system, in which the inactive copper atoms concentrate strongly in the surface, the addition of only a few percent of copper to nickel will markedly decrease the concentration of multiplet nickel atom sites. While such a geometric argument can account for a large inhibiting effect of copper on the hydrogenolysis activity of nickel, there is also the possibility that electronic interaction between copper and nickel may affect the catalysis. In view of the low ability of copper relative to nickel to chemisorb a variety of molecules, one might expect that addition of copper to nickel in an alloy would decrease the strength of adsorption of hydrocarbon species on the surface. In ethane hydrogenolysis, the strength of bonding between the two carbon atoms in the chemisorbed intermediate might be expected to vary in an

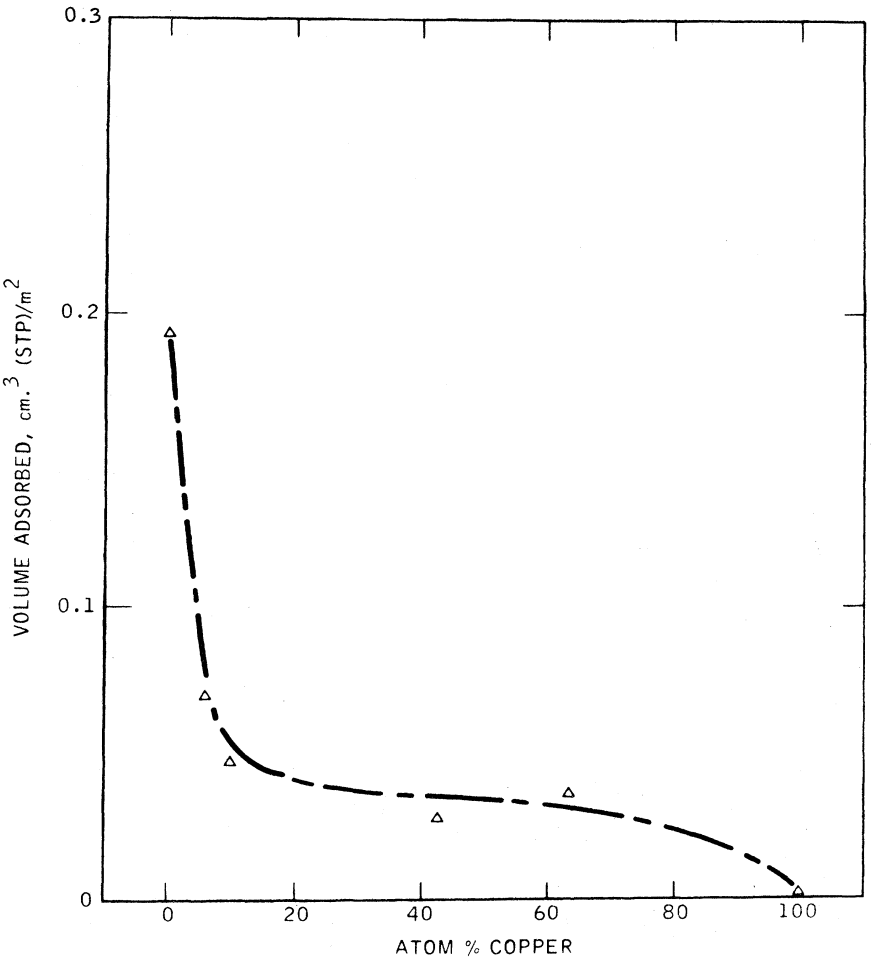

FIG. 11. The chemisorption of hydrogen on nickel–copper catalysts at room temperature as a function of composition. The chemisorbed hydrogen refers to the amount that is retained on the surface after 10 min evacuation at room temperature following completion of an adsorption isotherm (Sinfelt, 1974a; Sinfelt *et al.*, 1972).

inverse manner with the strength of bonding of the carbon atoms to the metal. One would then conclude that rupture of the carbon-carbon bond would be inhibited by a decrease in the strength of adsorption accompanying addition of copper to nickel. If carbon–carbon rupture is rate limiting, the rate of hydrogenolysis should then decrease.

In the case of cyclohexane dehydrogenation, a site consisting of a multiplet of active nickel atoms may not be necessary. While this hypothesis would account for the absence of a steep decline in activity as copper is added to nickel, it does not explain why copper-rich alloys have dehydrogenation activities as high as or higher than that of pure nickel. However, if the activity is controlled by a step whose rate is inversely related to the strength of adsorption (e.g., desorption of the benzene product), the addition of copper to nickel could increase the activity of a catalytic site and compensate for a decrease in the number of such sites. Over the range of composition from pure nickel to pure copper, however, the rate-determining step probably changes. For pure copper, the chemisorption of cyclohexane may be limiting.

The nickel–copper alloys discussed in the previous paragraphs were prepared under conditions of complete miscibility of the two components. It is also of interest to consider a system such as ruthenium–copper, the components of which are essentially completely immiscible in the bulk. The crystal structures of the two metals are different, ruthenium having a hexagonal close-packed structure and copper a face-centered cubic structure. Although the ruthenium–copper system can hardly be considered as one which forms alloys, bimetallic ruthenium–copper aggregates can be prepared which are similar to alloys such as nickel–copper in their catalytic behavior. In such aggregates, the copper tends to cover the surface of the ruthenium. Evidence for this comes from studies of hydrogen chemisorption capacity and ethane hydrogenolysis activity, both of which are markedly suppressed when even small amounts of copper are present with the ruthenium (Sinfelt *et al.*, 1976). Additional evidence is provided by electron spectroscopy (ESCA) studies, which tend to reflect the composition of the surface region of a material, extending to a depth of several layers of atoms. In Fig. 12 are shown ESCA data on bimetallic ruthenium–copper aggregates (Helms and Sinfelt, 1978). The surface areas of these aggregates were about 6.5 m^2/g. The ratio of the intensity of the copper $2p_{3/2}$ line of the spectrum to the intensity of the ruthenium $3d_{5/2}$ line is shown as a function of copper content. The dashed line shows the relationship expected if the ruthenium and copper were uniformly distributed throughout the samples. The solid curve shows the data actually obtained, and indicates a

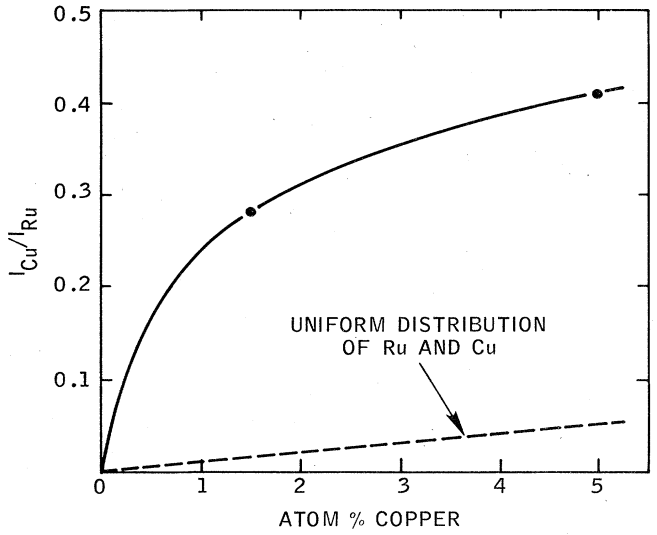

FIG. 12. Electron spectroscopy (ESCA) data on low-surface-area (~6.5 m^2/g) ruthenium–copper aggregates. The ratio I_{Cu}/I_{Ru} of the intensity of electron emission from the copper $2p_{3/2}$ level to that from the ruthenium $3d_{5/2}$ level is shown as a function of copper content. The dashed line represents the ratio expected for a uniform distribution of copper with ruthenium. The fact that the observed ratios are much higher than those of the dashed line indicates that the copper is located on the surface of the ruthenium, and that the degree of coverage of the ruthenium by the copper is high (Helms and Sinfelt, 1978).

much higher ratio of copper to ruthenium in the surface region than is indicated by the dashed line. The binding energies of the electrons in the $2p_{3/2}$ state of copper and the $3d_{5/2}$ state of ruthenium are, respectively, 932 and 284 eV. The kinetic energies of the ejected photoelectrons from the copper and ruthenium were approximately 550 and 1200 eV in the experiments. The effective escape depths of the electrons from the copper and ruthenium are estimated to be about 7 and 12 Å (with an uncertainty of about ±25%). Electron takeoff angles of 45° were employed in the experiments. The ESCA data show a good correlation with hydrogen chemisorption data (Fig. 13), an increase in the ratio I_{Cu}/I_{Ru} being accompanied by a decrease in hydrogen chemisorption (Helms and Sinfelt, 1978). The results of the ESCA experiments on the ruthenium–copper aggregates, in addition to the results of the chemisorption and catalysis experiments, suggest an interaction between the two components analogous to that which would exist in the chemisorption of copper on ruthenium. Thus, despite the fact that copper and ruthenium do not form solid solutions in the bulk, there is evidence of significant interaction between the two components at an interface.

As noted, the behavior of the ruthenium–copper system for ethane hydrogenolysis is similar to that observed for nickel–copper. In cyclohexane dehydrogenation to benzene, the behavior is again similar, in that copper has only a small effect on dehydrogenation activity. However, in the ruthenium–copper system

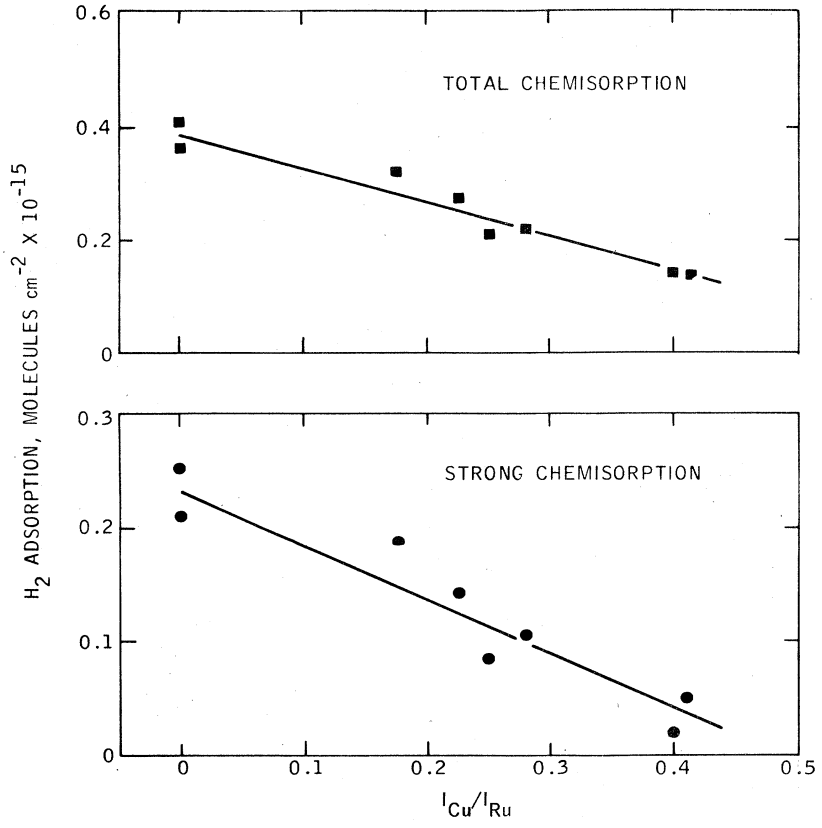

FIG. 13. Correlation of hydrogen chemisorption capacity of ruthenium–copper aggregates with the ratio I_{Cu}/I_{Ru} of the intensity of electron emission from the copper $2p_{3/2}$ level to that from the ruthenium $3d_{5/2}$ level (chemisorption data at room temperature). The upper part of the figure is the total chemisorption at 100 Torr equilibrium pressure. The lower part is the strong chemisorption, i.e., the amount which is not removed by evacuation to 10^{-6} Torr at room temperature. The samples were all heated in hydrogen at temperatures of 400°–600 °C and subsequently evacuated at elevated temperature prior to the ESCA and hydrogen chemisorption measurements (Helms and Sinfelt, 1978).

there is the additional feature that pure ruthenium exhibits extensive hydrogenolysis of cyclohexane to lower carbon number alkanes (mostly methane) in addition to dehydrogenation to benzene. Addition of copper to ruthenium suppresses hydrogenolysis strongly relative to dehydrogenation, so that a marked increase in the selectivity to benzene is observed. Different chemisorbed intermediates are probably involved in the dehydrogenation and hydrogenolysis reactions. By analogy with ethane hydrogenolysis, the intermediate in cyclohexane hydrogenolysis is probably a hydrogen deficient surface residue which forms bonds with more than one surface metal atom.

In general, the addition of a Group IB metal to a Group VIII metal decreases hydrogenolysis activity markedly, but has a much smaller effect on such other reactions as dehydrogenation, hydrogenation, and isomerization of hydrocarbons (Sinfelt *et al.*, 1969, 1971, 1972; Sinfelt, 1973b; Ponec and Sachtler 1972; Beelen *et al.*, 1973). Selectivity is therefore an important aspect of hydrocarbon conversion on bimetallic catalysts of this type.

B. Bimetallic cluster catalysts

The surface areas of bimetallic systems of the type considered in the previous section are too low for industrial catalytic applications, by about two orders of magnitude. A method of increasing the surface area of a metal is to disperse it on a carrier such as silica or alumina. The carrier itself has a high surface area, commonly in the range of 100–300 m^2/g. A supported bimetallic catalyst can be prepared simply by impregnating a carrier with an aqueous solution of salts of the two metals of interest. The material is dried and then contacted with a stream of hydrogen at elevated temperature to reduce the metal salts. This procedure results in the formation of very small metal clusters dispersed on the surface of the carrier. The nature of these clusters is the question of interest. Will the individual clusters be monometallic or will they contain atoms of both metals and therefore be bimetallic? On purely statistical grounds one might expect that the individual clusters would contain atoms of both metals. This expectation is supported by experiment, even for cases in which the individual metal components exhibit very low miscibility in the bulk (Sinfelt, 1973b). Examples of the latter type which have been investigated are ruthenium-copper and osmium-copper supported on silica, in which the metal clusters cover about 1% of the surface of the silica. The metal dispersion, expressed as the ratio of surface metal atoms to total metal atoms, is in the range 0.5–1 in these systems.

Although direct experimental verification of bimetallic clusters in such highly dispersed systems is difficult, a catalytic reaction can serve as a sensitive probe to obtain evidence of interaction between the atoms of the two metallic components. For supported bimetallic combinations of a Group VIII and a Group IB metal, the hydrogenolysis of ethane to methane is a very useful reaction for this purpose. In unsupported bimetallic systems of this type, the interaction between the Group VIII metal and the Group IB metal results in a marked inhibition of the hydrogenolysis activity of the former. In applying ethane hydrogenolysis as a probe to establish interaction between copper and either ruthenium or osmium on a carrier, one simply looks for a marked suppression of hydrogenolysis activity of the Group VIII metal when copper is present. Experiments of this type have demonstrated clearly that the metal components are not isolated from each other on the carrier, and therefore provide evidence for the existence of bimetallic clusters (Sinfelt, 1973b). Hydrogen chemisorption can be employed in a similar manner as a probe, in which case interaction of copper with either ruthenium or osmium is indicated by a suppression of chemisorption capacity. The utilization of hydrogen chemisorption and ethane hydrogenolysis as probes to detect bimetallic clusters is illustrated by the data on highly dispersed ruthenium-copper clusters in Figs. 14 and 15 (Sinfelt *et al.*, 1976).

It is interesting to consider how the state of dispersion of ruthenium–copper catalysts affects the relationship between hydrogen chemisorption capacity or ethane hydrogenolysis activity and catalyst composition. The data in Figs. 14 and 15 provide a comparison of large ruthenium–copper aggregates with highly dispersed ruthenium–copper clusters. The highly dispersed clusters require a much higher atomic ratio of copper to ruthenium than the large aggregates to achieve a given degree of inhibition of hydrogen chemisorption or ethane hydrogenolysis. The required ratios differ by a factor approximately equal to the ratio of the metal dispersions of the catalysts. This indicates that the copper in a ruthenium–copper aggregate is confined to the surface, which is consistent with the extremely low miscibility of the two metals in the bulk state. If one envisions a series of ruthenium–copper aggregates of varying size, each containing a monolayer of copper on the surface, the atomic ratio of copper to ruthenium in an aggregate will increase with decreasing aggregate size. When the aggregates become small enough, the atomic ratio of copper to ruthenium attains a value of the order of unity. The resulting ruthenium–copper entity is a model of a highly dispersed bimetallic cluster. Consequently, a highly dispersed bimetallic cluster may have compositions far outside the range of those possible in a bulk solid solution of the two metals.

As copper is incorporated with ruthenium or osmium in bimetallic clusters, the selectivity for conversion of cyclohexane to benzene is improved greatly, as shown in Fig. 16 (Sinfelt, 1973b). Hydrogenolysis to alkanes is inhibited markedly, while dehydrogenation to benzene is relatively unaffected. The behavior is similar to that already described for unsupported ruthenium-copper aggregates and provides further evidence for the interaction between copper and the Group VIII metal on the carrier.

The bimetallic clusters discussed thus far have been combinations of a Group VIII and a Group IB metal. These systems are good model systems for using chemisorption and catalysis as probes in investigating the bimetallic cluster concept. From the viewpoint of practical catalysis the obvious interest in this type of system is the improved selectivity for certain reactions, as a result of inhibition of hydrogenolysis. Another type

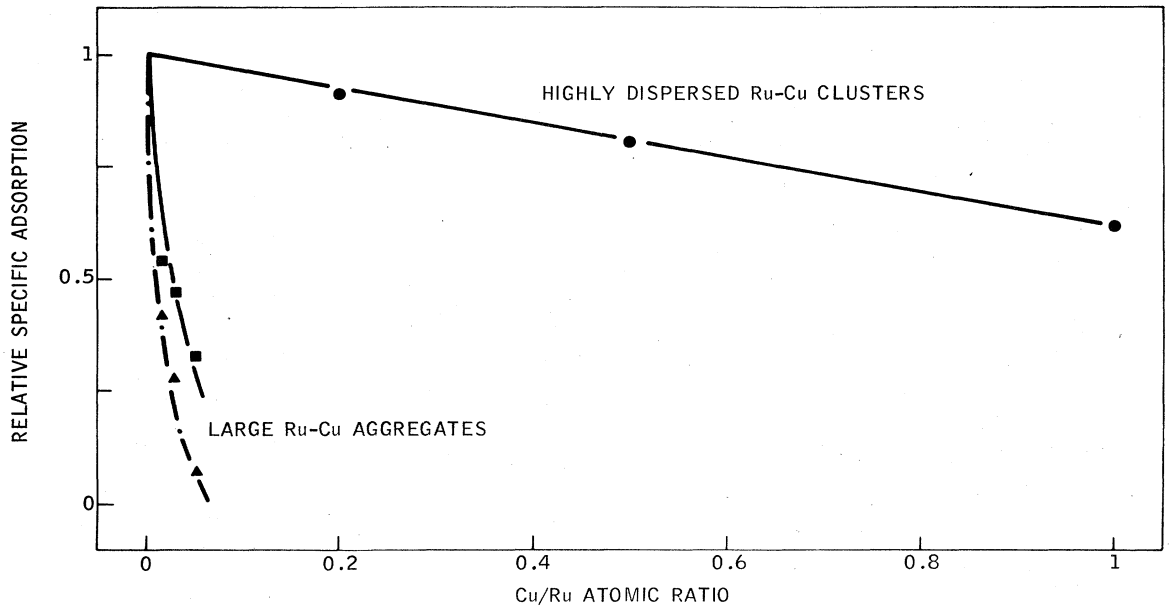

FIG. 14. Influence of the state of dispersion of ruthenium–copper catalysts on the relationship between hydrogen chemisorption capacity and catalyst composition. The large ruthenium–copper aggregates have a metal dispersion of the order of 1%, while the highly dispersed ruthenium–copper clusters have a metal dispersion of the order of 50%. The latter were supported on silica. In the case of the large ruthenium–copper aggregates, the square points represent total hydrogen chemisorption while the triangular points represent strongly chemisorbed hydrogen, the latter referring to hydrogen which can not be removed by evacuation at room temperature (Sinfelt *et al.*, 1976).

of bimetallic cluster of interest is a combination of atoms of two Group VIII metals, e.g., platinum–palladium, platinum–rhodium, or platinum–iridium (Sinfelt, 1976b). Bimetallic clusters of this type are of interest in the reforming of petroleum naphthas.

We select the platinum–iridium system for further discussion. Bimetallic clusters of platinum and iridium can be prepared by coimpregnating a carrier such as

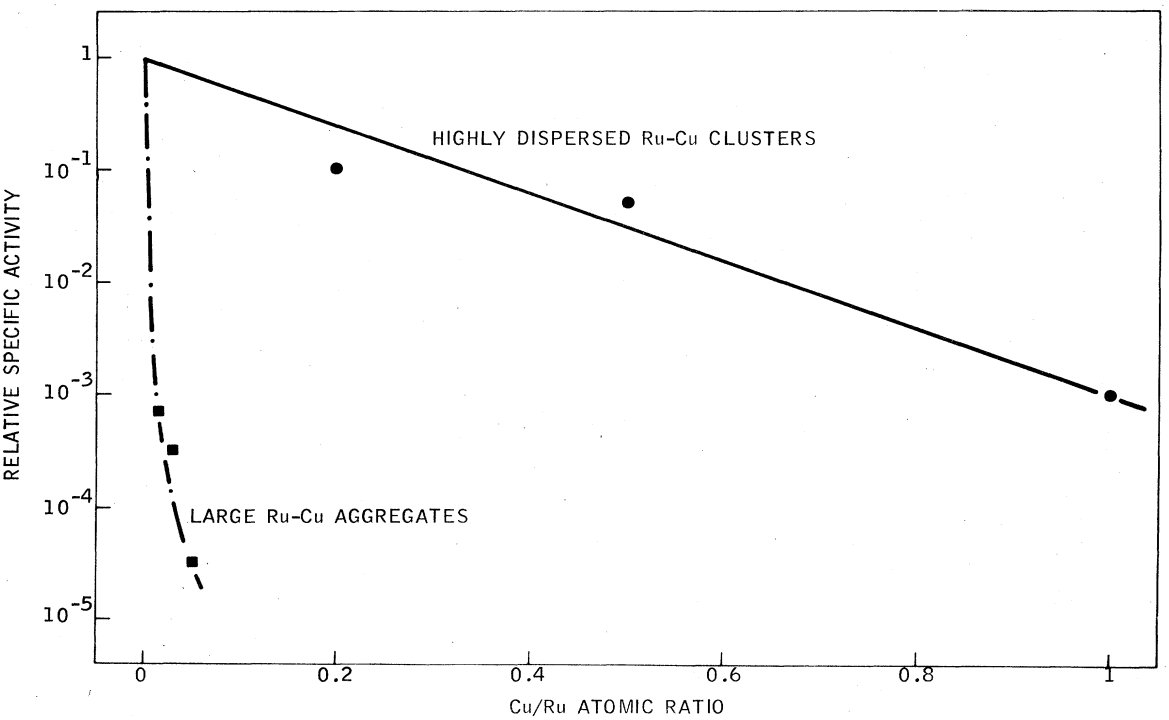

FIG. 15. Influence of the state of dispersion of ruthenium–copper catalysts on the relationship between ethane hydrogenolysis activity and catalyst composition. The catalysts are the same as in Fig. 14 (Sinfelt *et al.*, 1976).

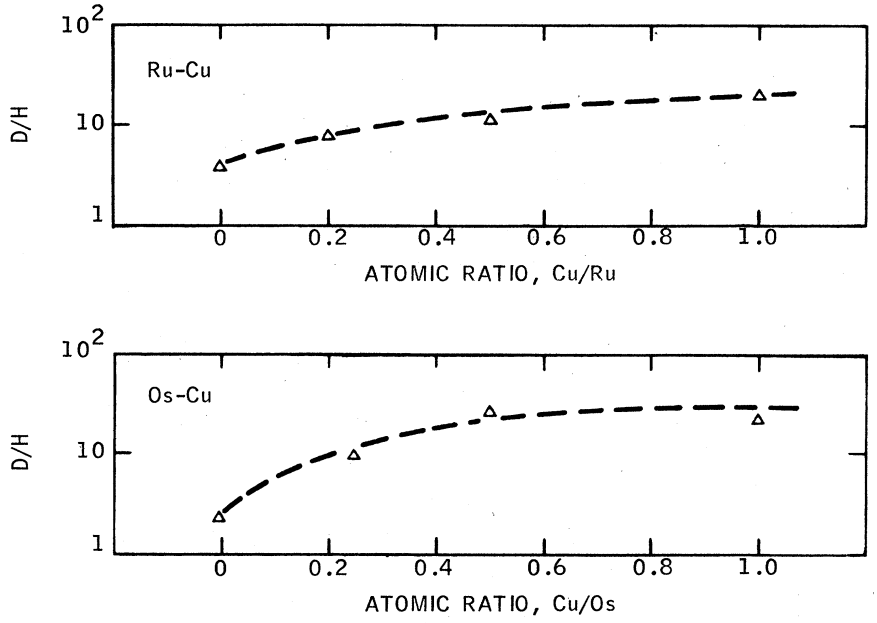

FIG. 16. Selectivity of conversion of cyclohexane over silica-supported bimetallic clusters of ruthenium–copper and osmium–copper at 316 °C. The selectivity is the ratio D/H, in which D is the rate of dehydrogenation of cyclohexane to benzene and H is the rate of hydrogenolysis to low-molecular-weight alkanes, primarily methane. The selectivity of either ruthenium or osmium is increased markedly when copper is added to form bimetallic clusters (Sinfelt, 1973b).

silica or alumina with an aqueous solution of chloroplatinic and chloroiridic acids. After the impregnated carrier is dried and possibly calcined at mild conditions (250 °–300 °C), it is reduced in flowing hydrogen at an elevated temperature (300 °–500 °C). Some idea of the variation of metal dispersion with variation of the total metal content of such catalysts can be obtained from the data on hydrogen chemisorption shown in Fig. 17 (Sinfelt and Via, 1979). All of the catalysts in the figure contain equal fractions by weight of platinum and iridium (corresponding to a Pt/Ir atomic ratio very close to unity). Data are shown for platinum–iridium clusters supported on both alumina and silica, the surface areas of which are, respectively, about 200 and 300 m^2/g. The data represent strongly chemisorbed hydrogen, i.e., the amount of chemisorbed hydrogen which can not be removed by evacuation at room temperature to approximately 10^{-6} Torr. The amount ad-

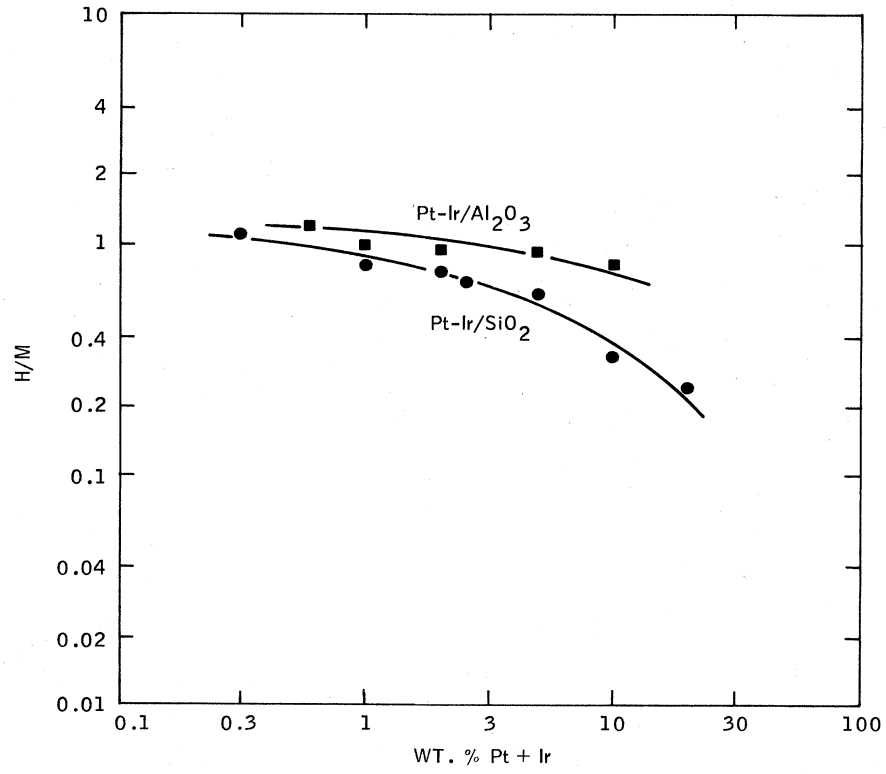

FIG. 17. Hydrogen chemisorption at room temperature on platinum–iridium catalysts as a function of the platinum plus iridium content. All the catalysts contain equal percentages by weight of platinum and iridium. The quantity H/M represents the ratio of the number H of hydrogen atoms adsorbed to the number M of metal atoms (platinum and iridium) in the catalyst, and refers to the amount of hydrogen retained by the catalyst when the adsorption cell is evacuated at room temperature for 10 min after completion of the adsorption isotherm; i.e., the H/M values represent the strongly chemisorbed fraction. The upper curve is for alumina-supported platinum–iridium clusters while the lower curve is for silica-supported clusters (Sinfelt 1976b; Sinfelt and Via, 1979).

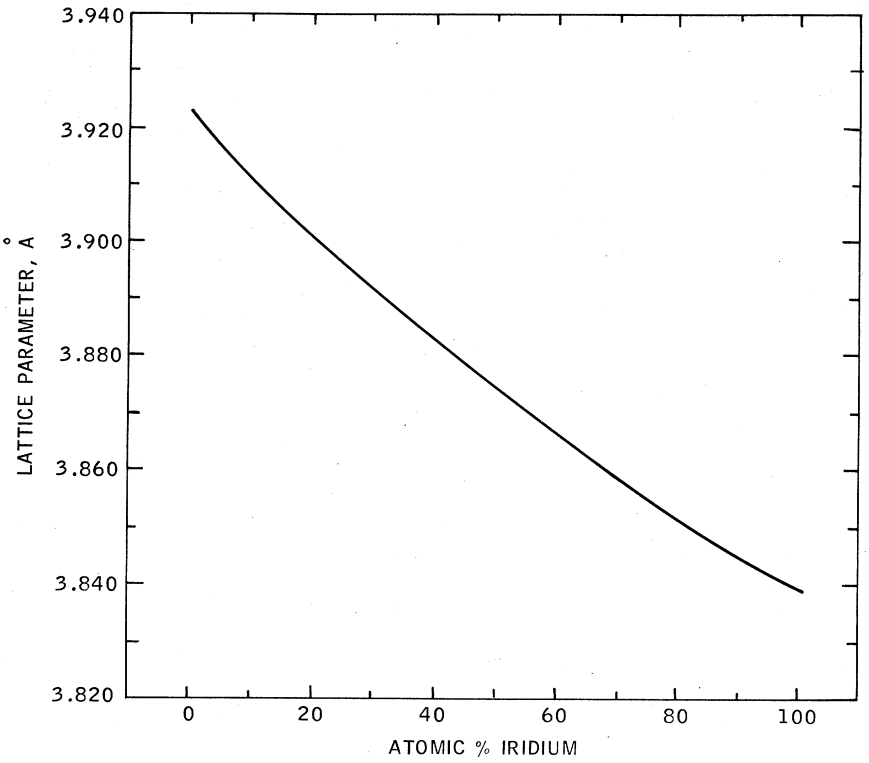

FIG. 18. Lattice parameter of platinum-iridium solid solutions as a function of composition (data from Pearson, 1964).

sorbed is expressed in terms of the quantity H/M, which represents the ratio of the number of hydrogen atoms adsorbed to the number of metal atoms (platinum and iridium) in the catalyst. Values of H/M are consistently higher for alumina-supported platinum-iridium than for silica-supported platinum-iridium, indicating higher metal dispersion on alumina. We see that H/M appears to approach a limiting value near unity as the metal concentration is decreased below about 1 wt.%. At these low metal concentrations essentially all of the platinum and iridium atoms are surface atoms. Electron microscopy data on such catalysts show the average diameters of the metal clusters to be of the order of 10 Å or lower. Clusters of this size necessarily consist almost exclusively of surface atoms. The stoichiometry of the strongly chemisorbed fraction therefore corresponds closely to one hydrogen atom per surface metal atom. Thus the value of H/M for the strongly chemisorbed fraction is taken as a direct measure of the dispersion, which is defined as the ratio of surface atoms to total atoms in the metal clusters.

X-ray diffraction data were obtained on some of the platinum–iridium catalysts. Both platinum and iridium crystallize as fcc structures, and they form solid solutions in all proportions in the bulk (Pearson, 1964). The lattice parameter is a function of the composition of the solid solution, as shown in Fig. 18 (Sinfelt and Via, 1979; data obtained from Pearson, 1964). Thus measurements of lattice parameters provide a way of demonstrating the presence of bimetallic clusters of platinum and iridium in the catalysts. The interpretation of x-ray diffraction data is relatively straightforward for silica-supported platinum–iridium clusters because the diffraction pattern of the silica does not interfere significantly with the diffraction pattern of the clusters. X-ray diffraction data on a silica-supported platinum–iridium catalyst containing 10 wt.% platinum and 10 wt.% iridium are shown in the middle field of Fig. 19 (Sinfelt and Via, 1979). The metal dispersion of the catalyst as determined by hydrogen chemisorption is 0.24. A portion of the diffraction pattern is shown which includes the (220) reflection. The upper field of the figure shows the corresponding part of the diffraction pattern of a physical mixture of bulk platinum and bulk iridium diluted with silica. In the lower field of the figure is shown the same region of the diffraction pattern for a physical mixture of equal weights of silica-supported platinum and silica-supported iridium, the mixture containing the same absolute amounts of platinum and iridium as the platinum–iridium bimetallic catalyst sample. It should be noted that the platinum–iridium bimetallic catalyst was diluted with an equal weight of silica. The background scattering arising from the silica carrier was subtracted from the total scattering in the diffraction patterns for the catalysts.

In considering the diffraction patterns in Fig. 19, we see that the platinum–iridium bimetallic clusters give a single diffraction line (middle field of figure) about midway between the lines (upper field of figure) for bulk platinum and bulk iridium. The line for the clusters is broader than the lines for the bulk metals because of the small size of the clusters. Using the Scherrer equation (Klug and Alexander, 1974), we calculate an average platinum–iridium cluster size of 49 Å from the line width. The lattice parameter of the platinum–iridium clusters is 3.875 Å, as determined from the positions of a number of lines in the diffraction pattern. This value corresponds to a composition of 50% iridium in

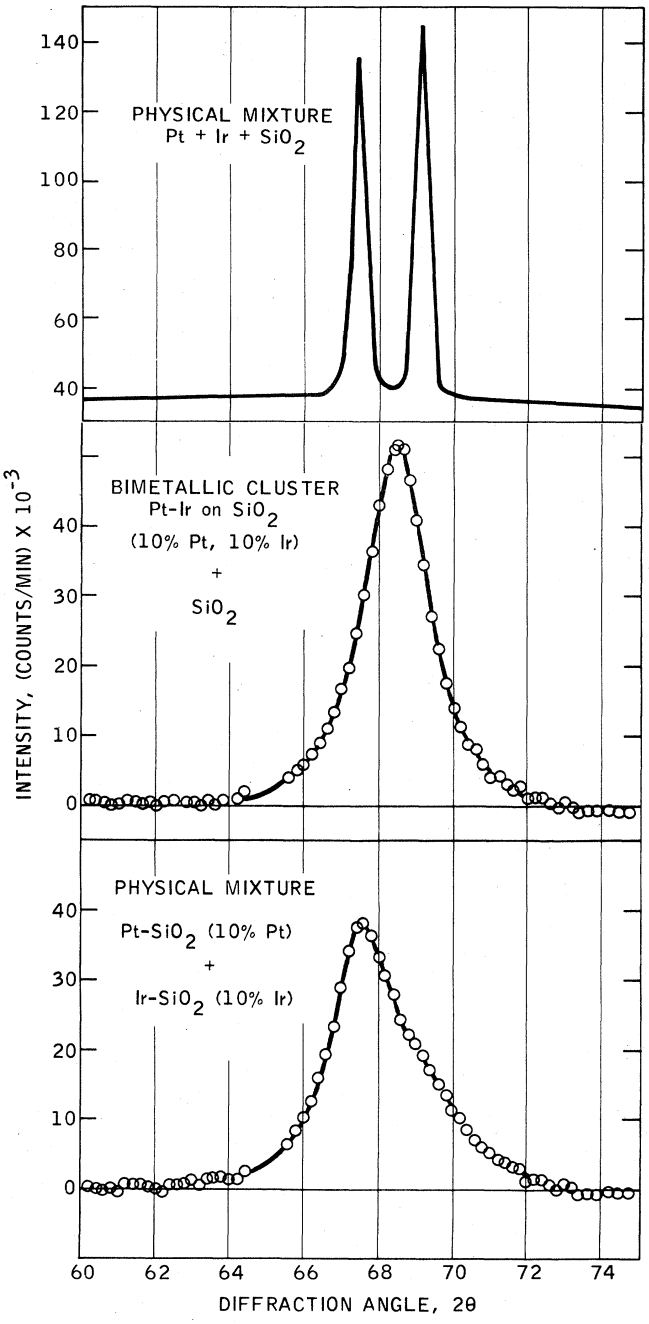

FIG. 19. X-ray diffraction study of a platinum-iridium bimetallic cluster catalyst. The upper field is a reference pattern for a physical mixture of platinum and iridium metals diluted with silica. The middle field is a pattern for a silica-supported platinum–iridium bimetallic cluster catalyst containing 10 wt. % Pt and 10 wt. % Ir, mixed with an equal weight of silica. The lower field is a pattern for a physical mixture of silica-supported Pt clusters and silica-supported Ir clusters, the catalysts containing 10 wt. % Pt and 10 wt. % Ir, respectively. The mixture was formulated to match the platinum and iridium contents of the sample in the middle field of the figure (Sinfelt, 1976b; Sinfelt and Via, 1979).

Fig. 18, in agreement with the overall composition. The diffraction pattern of the physical mixture of silica-supported platinum clusters and iridium clusters in the lower field of the figure consists of overlapping lines for the two individual types of clusters, and is clearly different from that of the platinum–iridium bimetallic clusters. The overlapping is due to the broadened nature of the individual lines resulting from the small sizes of the individual clusters of platinum and iridium, estimated to be 56 and 27 Å, respectively, from x-ray diffraction data on the individual catalysts.

X-ray diffraction has proved to be useful for the investigation of silica-supported platinum–iridium clusters with metal dispersions as high as 0.60 (Sinfelt, 1976b; Sinfelt and Via, 1979). For platinum–iridium clusters of higher dispersion, the application of x-ray diffraction becomes very difficult, as it does for supported metal catalysts of any kind having such high dispersions. The lines in the diffraction patterns are then extremely broad and weak, becoming indistinguishable from the background. To obtain structural information on the more highly dispersed clusters, we are now obtaining data on the extended x-ray absorption fine structure (EXAFS) of the catalysts.

In the preparation of the highly dispersed platinum–iridium bimetallic clusters described here, the carrier (SiO_2 or Al_2O_3) is first coimpregnated with chloroplatinic and chloroiridic acids and then dried at a temperature of 110 °C prior to reduction in hydrogen at 500 °C. If the catalyst is heated in air (calcined) at too high a temperature, say 500 °C, the iridium undergoes oxidation and agglomeration to form large crystallites of IrO_2. On subsequent reduction in hydrogen at 500 °C, the IrO_2 crystallites are reduced to large metallic iridium crystallites (>200 Å size). At this point, the material consists of a mixture of a highly dispersed platinum or platinum-rich phase and large crystallites of iridium. The diffraction profile for the (220) region for this material is given in the upper field of Fig. 20 (Sinfelt and Via, 1979). The contrast between this pattern and the pattern for platinum–iridium bimetallic clusters in the lower field of Fig. 20 is clear. These results demonstrate the importance of preparative conditions in the formation of bimetallic clusters in the platinum–iridium system. In general, exposure to air at temperatures below about 375 °C does not appear to be harmful, but contact with air at temperatures above about 450 °C should be avoided (Sinfelt, 1976b).

V. CONCLUSION

It has been difficult for the science of catalysis to keep pace with the enormous technological advances in the field. The complexity of catalytic phenomena and our limitations in ability to obtain information at a sufficiently microscopic level are important factors contributing to this problem. Nevertheless, significant progress is being made. In the area of metal catalysts, for example, important advances in our knowledge of the structure of highly dispersed systems of technological interest are resulting from new developments in ex-

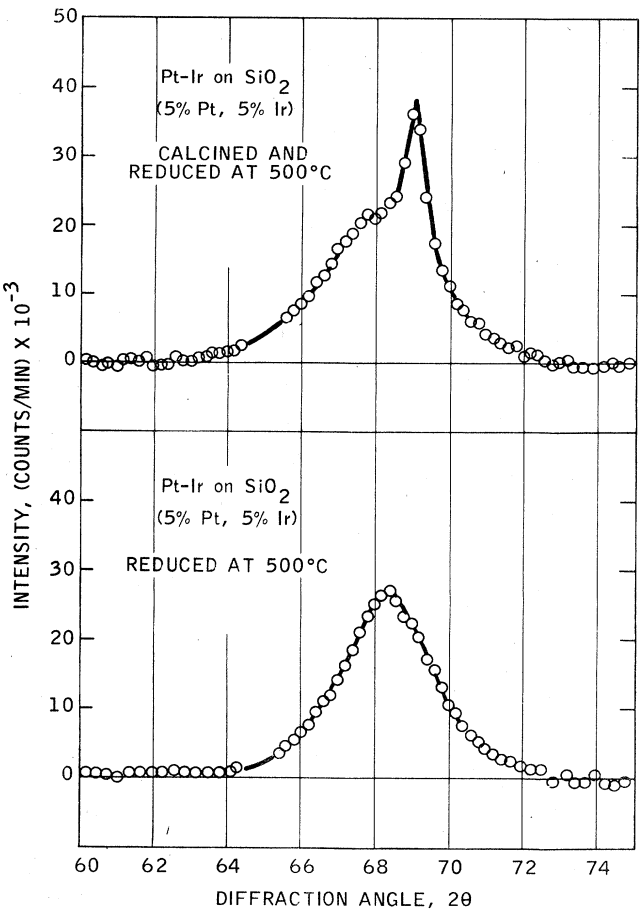

FIG. 20. X-ray diffraction pattern on a silica-supported platinum–iridium sample heated in air at 500 °C prior to reduction in hydrogen at 500 °C (upper field of figure), indicating a mixture of large iridium crystallites and much smaller platinum clusters. A diffraction pattern on a silica-supported platinum–iridium bimetallic cluster catalyst of the same composition is shown in the lower field for comparison. The catalyst in the lower field had not been exposed to air at high temperature prior to reduction, which illustrates the importance of the preparative conditions in the formation of highly dispersed platinum–iridium bimetallic clusters. The data are for samples containing 5 wt. % each of platinum and iridium, corresponding to a platinum–iridium atomic ratio very close to 1 (Sinfelt, 1976b; Sinfelt and Via, 1979).

perimental methods such as high-resolution electron microscopy and extended x-ray absorption fine structure (EXAFS). The exploitation of these modern developments, in conjunction with the more traditional approaches using selective chemisorption and model catalytic reactions as probes, has introduced some intriguing features related to the science of highly dispersed metals.

Concurrent with the progress being made in our understanding of metal catalysts, advances in the development of new catalyst systems continue to appear. An example is the development of bimetallic (or, more generally, polymetallic) cluster catalysts which have found extensive application in petroleum refining for the production of high "antiknock" components for gasoline (Sinfelt, 1972b, 1976a). The developments in this area provide an example of advances in catalyst technology which have evolved within a framework of research directed toward an improved understanding of catalytic phenomena.

Adler, S., and J. J. Keavney, 1960, J. Phys. Chem. **64**, 208.
Ahern, S. A., M. J. C. Martin, and W. Sucksmith, 1958, Proc. R. Soc. A **248**, 145.
Ashley, C. A., and S. Doniach, 1975, Phys. Rev. B **11**, 1279.
Balandin, A. A., 1958, Adv. Catal. Relat. Subj. **10**, 96.
Bean, C. P., and J. D. Livingston, 1959, J. Appl. Phys. **30**, 120S.
Beelen, J. M., V. Ponec, and W. M. H. Sachtler, 1973, J. Catal. **28**, 376.
Bender, M. L., and L. J. Brubacher, 1973, *Catalysis and Enzyme Action* (McGraw-Hill, New York).
Best, R. J., and W. W. Russell, 1954, J. Am. Chem. Soc. **76**, 838.
Boudart, M., 1968, *Kinetics of Chemical Processes* (Prentice-Hall, Englewood Cliffs, N. J.), p. 61.
Brown, H. C., and C. A. Brown, 1962, J. Am. Chem. Soc. **84**, 1493.
Brunauer, S., P. H. Emmett, and E. Teller, 1938, J. Am. Chem. Soc. **60**, 309.
Cadenhead, D. A., and N. J. Wagner, 1968, J. Phys. Chem. **72**, 2775.
Carter, J. L., J. A. Cusumano, and J. H. Sinfelt, 1971, J. Catal. **20**, 223.
Carter, J. L., and J. H. Sinfelt, 1966, J. Phys. Chem. **70**, 3003.
Cimino, A., M. Boudart, and H. S. Taylor, 1954, J. Phys. Chem. **58**, 796.
Coles, B. R., 1956, J. Inst. Met. **84**, 346.
Dowden, D. A., 1950, J. Chem. Soc. 242.
Eisenberger, P., B. Kincaid, S. Hunter, D. Sayers, E. Stern, and F. W. Lytle, 1974, Proceedings of the IV International Conference on Vacuum U. V. Radiation Physics, Hamburg, July 22–26, 1974 (Pergamon, London), p. 806.
Emmett, P. H., and N. Skau, 1943, J. Am. Chem. Soc. **65**, 1029.
Emmett, P. H., and S. Brunauer, 1937, J. Am. Chem. Soc. **59**, 310.
Frankenburg, W. G., 1955, in *Catalysis*, edited by P. H. Emmett (Reinhold, New York), Vol. III, p. 171.
Gruber, H., 1962, J. Phys. Chem. **66**, 48.
Haensel, V., 1949a, U. S. Patent 2,479,109.
Haensel, V., 1949b, U. S. Patent 2,479,110.
Haensel, V., and G. R. Donaldson, 1951, Ind. Eng. Chem. **43**, 2102.
Hall, W. K., and P. H. Emmett, 1958, J. Phys. Chem. **62**, 816.
Hall, W. K., and P. H. Emmett, 1959, J. Phys. Chem., **63**, 1102.
Helms, C. R., 1975, J. Catal. **36**, 114.
Helms, C. R., and J. H. Sinfelt, 1978, Surf. Sci. **72**, 229.
Kincaid, B. M., 1975, Ph.D. dissertation, Stanford University.
Kincaid, B. M., 1977, J. Appl. Phys. **48**, 2684.
Kincaid, B. M., and P. Eisenberger, 1975, Phys. Rev. Lett. **34**, 1361.
Klug, H. P., and L. E. Alexander, 1974, *X-Ray Diffraction Procedures for Polycrystalline and Amorphous Materials* (Wiley, New York), 2nd edition, p. 656.
Kokes, R. J., and P. H Emmett, 1959, J. Am. Chem. Soc. **81**, 5032.
Kronig, R. de L., 1931, Z. Phys. **70**, 317.
Kronig, R. de L., 1932a, Z. Phys. **75**, 191.
Kronig, R. de L., 1932b, Z. Phys. **75**, 468.
Lee, P. A., and G. Beni, 1977, Phys. Rev. B **15**, 2862.
Lee, P. A., and J. B. Pendry, 1975, Phys. Rev. B **11**, 2795.

Lytle, F. W., 1965, in *Physics of Non-Crystalline Solids*, edited by J. A. Prins (North-Holland, Amsterdam), p. 12.
Lytle, F. W., 1966, in *Advances in X-ray Analysis*, edited by G. R. Mallett, M. Fay, and W. M. Mueller (Plenum, New York), p. 398.
Lytle, F. W., D. Sayers, and E. Stern, 1975, Phys. Rev. B **11**, 4825.
Lytle, F. W., G. H. Via, and J. H. Sinfelt, 1977, J. Chem. Phys. **67**, 3831.
McKee, D. W., 1965, Trans. Faraday Soc. **61**, 2273.
McKee, D. W., 1967, J. Catal. **8**, 240.
Murphree, E. V., C. L. Brown, H. G. M. Fischer, E. J. Gohr, and W. J. Sweeney, 1943, Ind. Eng. Chem. **35**, 768.
Pearson, W. B., 1964, *A Handbook of Lattice Spacings and Structures of Metals and Alloys* (Pergamon, London), p. 704.
Ponec, V., and W. M. H. Sachtler, 1972, J. Catal. **24**, 250.
Prestridge, E. B., G. H. Via, and J. H. Sinfelt, 1977, J. Catal. **50**, 115.
Prestridge, E. B., and D. J. C. Yates, 1971, Nature (Lond.) **234**, 345.
Prettre, M., 1963, *Catalysis and Catalysts*, translated by David Antin (Dover, New York), pp. 69–81.
Raney, M., 1940, Ind. Eng. Chem. **32**, 1199.
Rideal, E. K., 1968, *Concepts in Catalysis* (Academic, London), pp. 4–42.
Sachtler, W. M. H., and P. van der Plank, 1969, Surf. Sci. **18**, 62.
Sayers, D. E., 1971, Ph.D. dissertation, University of Washington.
Sayers, D. E., F. W. Lytle, and E. A. Stern, 1970, Adv. X-ray Anal. **13**, 248.
Sayers, D. E., F. W. Lytle, and E. A. Stern, 1971, Phys. Rev. Lett. **27**, 1204.
Schwab, G. M., 1950, Discuss. Faraday Soc. **8**, 166.
Selwood, P. W., 1956, *Magnetochemistry* (Interscience, New York), 2nd edition, pp. 374–408.
Selwood, P. W., 1962, *Adsorption and Collective Paramagnetism* (Academic, New York).
Sinfelt, J. H., 1964, J. Phys. Chem. **68**, 344.
Sinfelt, J. H., 1969, Catal. Rev. **3**(2), 175.
Sinfelt, J. H., 1972a, Annu. Rev. Mater. Sci. **2**, 641.
Sinfelt, J. H., 1972b, in Chem. Eng. News (July 3, 1972 issue) **50**, 18.
Sinfelt, J. H., 1972c, J. Catal. **27**, 468.
Sinfelt, J. H., 1973a, Adv. Catal. **23**, 91.
Sinfelt, J. H., 1973b, J. Catal. **29**, 308.
Sinfelt, J. H., 1974a, Catal. Rev.-Sci. Eng. **9**(1), 147.
Sinfelt, J. H., 1974b, Crit. Rev. Solid State Sci. **4**, 311.
Sinfelt, J. H., 1975, Prog. Solid State Chem. **10**(2), 55.
Sinfelt, J. H., 1976a, Platinum Metals Review **20**(4), 114.
Sinfelt, J. H., 1976b, U. S. Patent 3,953,368.
Sinfelt, J. H., 1977a, Acc. Chem. Res. **10**, 15.
Sinfelt, J. H., 1977b, Science **195**, 641.
Sinfelt, J. H., A. E. Barnett, and J. L. Carter, 1971, U. S. Patent 3,617,518.
Sinfelt, J. H., A. E. Barnett, and G. W. Dembinski, 1969, U. S. Patent 3,442,973.
Sinfelt, J. H., J. L. Carter, and D. J. C. Yates, 1972, J. Catal. **24**, 283.
Sinfelt, J. H., Y. L. Lam, J. A. Cusumano, and A. E. Barnett, 1976, J. Catal. **42**, 227.
Sinfelt, J. H., and G. H. Via, 1979, J. Catal. **56**, 1.
Sinfelt, J. H., G. H. Via, and F. W. Lytle, 1978, J. Chem. Phys. **68**, 2009.
Sinfelt, J. H., and D. J. C. Yates, 1967, J. Catal. **8**, 82.
Sinfelt, J. H., and D. J. C. Yates, 1968, J. Catal. **10**, 362.
Spenadel, L., and M. Boudart, 1960, J. Phys. Chem. **64**, 204.
Stern, E. A., 1974, Phys. Rev. B **10**, 3027.
Stern, E. A., D. E. Sayers, and F. W. Lytle, 1975, Phys. Rev. B **11**, 4836.
Taylor, W. F., and J. H. Sinfelt, 1967, U. S. Patent 3,320,182.
Thomson, S. J., and G. Webb, 1968, *Heterogeneous Catalysis* (Wiley, New York).
van der Plank, P., and W. M. H. Sachtler, 1967, J. Catal. **7**, 300.
Voge, H., and C. R. Adams, 1967, Adv. Catal. Relat. Subj. **17**, 151.
Watt, G. W., W. F. Roper, and S. G. Parker, 1951, J. Am. Chem. Soc. **73**, 5791.
Weisz, P. B., and C. D. Prater, 1954, Adv. Catal. **6**, 143.
Wheeler, A., 1955, in *Catalysis*, edited by P. H Emmett (Reinhold, New York), Vol. II, p. 105.
Wilson, G. R., and W. K. Hall, 1970, J Catal. **17**, 190.
Yates, D. J. C., and J. H. Sinfelt, 1967, J. Catal. **8**, 348.
Yates, D. J. C., W. F. Taylor, and J. H. Sinfelt, 1964, J. Am. Chem. Soc. **86**, 2996.

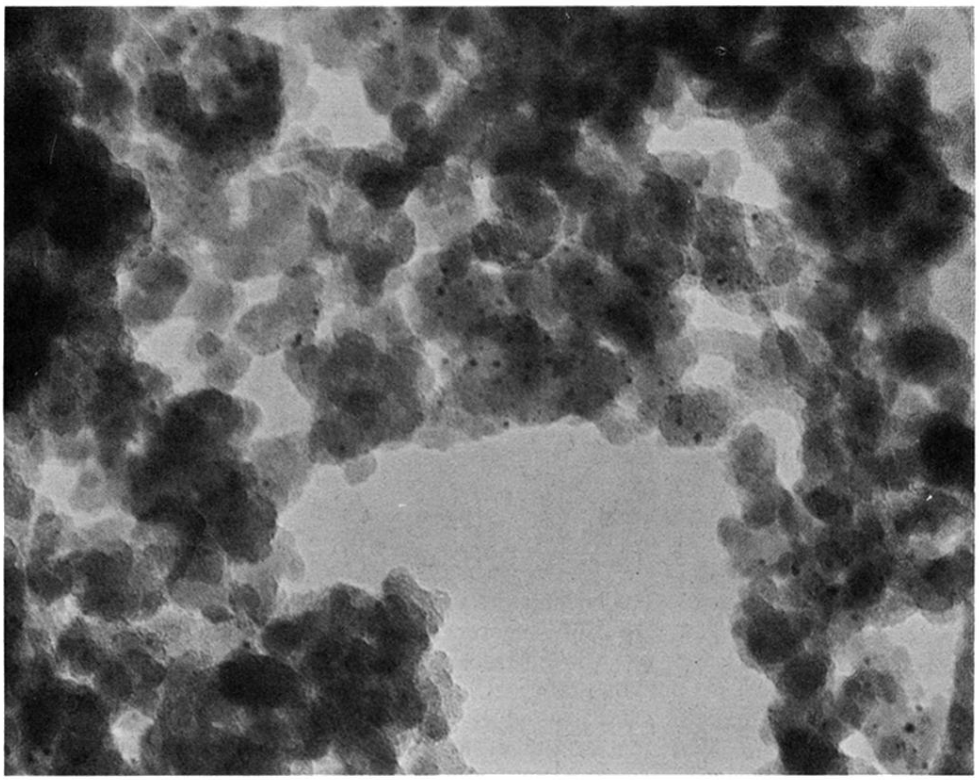

FIG. 2. Electron micrograph of silica-supported osmium catalyst containing 1 wt.% osmium. The osmium clusters (the black dots in the micrograph) are very highly dispersed, with diameters ranging from 5 to 25 Å. The average diameter is 12 Å (Prestridge, Via, and Sinfelt, 1977).